DOE/MC/30127 -- 5793
(DE97005490)

Solid-State 13C NMR Analysis of Shales and Coals From Laramide Basins

Final Report
March 1, 1995 - March 31, 1996

By:
Francis P. Miknis
Zun S. Jiao
Hanqing Zhao
Ronald C. Surdam

Work Performed Under Contract No.: DE-FC21-93MC30127

For
U.S. Department of Energy
Office of Fossil Energy
Federal Energy Technology Center
Morgantown Site
P.O. Box 880
Morgantown, West Virginia 26507-0880

By
Western Research Institute
365 North Ninth Street
Laramie, Wyoming 82070

Disclaimer

ACKNOWLEDGEMENT AND DISCLAIMER

This report was prepared with the support of the U.S. Department of Energy (DOE), Morgantown Energy Technology Center, under Cooperative Agreement Number DE-FC-93MC30127 and the Gas Research Institute (GRI) under contract GRI-5089-260-1894. However, any opinions, findings, conclusions, or recommendations expressed herein are those of the authors and do not necessarily reflect the views of the DOE or GRI.

TABLE OF CONTENTS

TABLE OF CONTENTS

LIST OF TABLES

LIST OF FIGURES

LIST OF FIGURES, Cont.

Figure

EXECUTIVE SUMMARY

This Western Research Institute (WRI) jointly sponsored research (JSR) project augmented and complemented research conducted by the University of Wyoming Institute For Energy Research for the Gas Research Institute. The project, "A New Innovative Exploitation Strategy for Gas Accumulations Within Pressure Compartments," was a continuation of a project funded by the GRI Pressure Compartmentalization Program that began in 1990. That project, "Analysis of Pressure Chambers and Seals in the Powder River Basin, Wyoming and Montana," characterized a new class of hydrocarbon traps, the discovery of which can provide an impetus to revitalize the domestic petroleum industry.

In support of the UW Institute For Energy Research's program on pressure compartmentalization, solid-state ^{13}C NMR measurements were made on sets of shales and coals from different Laramide basins in North America. NMR measurements were made on samples taken from different formations and depths of burial in the Alberta, Bighorn, Denver, San Juan, Washakie, and Wind River basins. The carbon aromaticity determined by NMR was shown to increase with depth of burial and increased maturation. In general, the NMR data were in agreement with other maturational indicators, such as vitrinite reflectance, illite/smectite ratio, and production indices. NMR measurements were also obtained on residues from hydrous pyrolysis experiments on Almond and Lance Formation coals from the Washakie Basin. These data were used in conjunction with mass and elemental balance data to obtain information about the extent of carbon aromatization that occurs during artificial maturation. The data indicated that 41 and 50% of the original aliphatic carbon in the Almond and Lance coals, respectively, aromatized during hydrous pyrolysis.

Because of the similarity of the work, this report combines Task 012 "Solid-State NMR Analysis of Naturally and Artificially Matured Kerogens" and Task 017 "Solid-State NMR Analysis of Mowry Shale From Different Sedimentary Basins" into one final topical report. The work was performed under the U.S. Department of Energy Cooperative Agreement, DE-FC21-93MC30127.

INTRODUCTION

Increasing costs and diminishing returns from oil and gas exploration threaten the nation's long-term energy security and international competitiveness. New approaches and supporting technology are needed to reverse these negative trends which presently characterize the domestic oil and gas industry. The discovery of subsurface fluid or pressure chambers has the potential to delineate a new class of hydrocarbon traps, thereby revitalizing interest in domestic exploration. To derive the benefits from pressure compartmentalization in petroleum exploration, the mechanisms for chamber formation must be understood.

The University of Wyoming (UW) Institute For Energy Research (IER), through funding by the Gas Research Institute (GRI), has initiated a multidisciplinary research program aimed at the development of a conceptual model of the formation, distribution, and destruction of pressure chambers and seals in sedimentary basins characterized by dynamic burial and erosional histories. This research began in 1990 and focused on the Powder River Basin (Wyoming and Montana), because this basin is known to have numerous and diverse types of pressure chambers. The main goals of the first phase of the research program were to document the presence of pressure chambers and seals, to characterize the pressure compartments and bounding seals, and to develop and validate a conceptual model for formation, distribution, and destruction of pressure compartments. A secondary goal was to use this information to design and interpret seismic experiments for detecting pressure chambers.

A major task of the IER research program is to evaluate the petrographic, diagenetic, and geochemical aspects of pressure chamber genesis. This task involves, *inter alia*, development of kinetic models that can be used to reconstruct the diagenetic and maturational history of pressure chambers. A key to understanding the diagenetic and maturational behavior is knowledge of the organic carbon structure of the kerogen in petroleum source rocks and how the kerogen structure changes during petroleum generation and during anomalous pressurization (pressure compartmentalization).

During the previous JSR project, Western Research Institute (WRI) performed solid-state ^{13}C and ^{29}Si NMR analyses on a suite of Mowry Formation shales from the Powder River Basin in Wyoming. The solid-state NMR measurements provided important information on the diagenesis and maturation of shales (Miknis 1992a, Miknis et al. 1993, MacGowan et al. 1994). The NMR results showed that the Mowry shale had little capacity to generate petroleum beyond a present-day depth of burial of ~8,000 ft. These results supported other geochemical analyses that were acquired on the suite of samples. The NMR data were combined with Rock-Eval data to estimate the hydrogen

budget for petroleum generation using a recently developed methodology (Patience et al. 1992, Miknis et al. 1993).

The IER's contract with the Gas Research Institute was renewed for a three-year period beginning in May 1993. This contract and Western Research Institute's cooperative agreement with the U.S. Department of Energy, DE-FC21-93MC30127, provided funding for WRI to continue NMR analysis and interpretation of kerogen maturation during the second phase of the IER project. WRI provided solid-state ^{13}C NMR analyses and services in support of the multidisciplinary analysis of pressure chambers in different Laramide basins. The NMR measurements provide a direct measurement of the aliphatic and aromatic carbon distributions in shales and coals. Monitoring these distributions as a function of temperature, either during artificial maturation, as in laboratory hydrous pyrolysis experiments, or naturally, as from depth of burial, provides information about the mechanisms of hydrocarbon generation. Such information is difficult, if not impossible, to obtain using other techniques. This information can then be used to place lower limits on depth of burial for the generation of oil and gas in sedimentary basins.

Additional NMR measurements and techniques were also employed to obtain information about chemical changes in sedimentary organic matter that occurs during artificial and natural maturation. Solid-state ^{13}C NMR measurements were combined with elemental analysis and mass balance data to determine the amount of aromatization of aliphatic carbon moieties that occurs during hydrous pyrolysis of coals from the Washakie Basin. Preliminary measurements using dipolar dephasing NMR techniques were also made to obtain estimates of the changes in the size of the fused aromatic ring system of coals during artificial and natural maturation.

EXPERIMENTAL

Samples

Solid-state ^{13}C NMR measurements were made on coals and carbonaceous shales obtained from different well locations in the Bighorn, Wind River, Denver, Alberta, San Juan, and Washakie Basins (Figure 1). Summary data are given in Tables 1-7. The coal samples used for the hydrous pyrolysis experiments were obtained from the Black Butte mine located about 10 miles east of Rock Springs, Wyoming. The coals were from the Almond and Lance Formations, Washakie Basin, and are of subbituminous rank. Both coal formations are being mined at the same surface mine.

Table 1. Summary of NMR Analyses of Mowry Formation, Bighorn Basin Shales

Sample	Depth, ft	%TOC	Aromaticity
B-31	1,100	2.0	0.32
B-5	3,015	0.7	0.56
B-32	4,215	1.9	0.54
B-8	4,530	1.1	0.57
B-34	5,980	1.6	0.49
B-35	6,293	1.4	--
B-36	7,365	1.5	0.5
B-15	8,010	1.2	0.82
B-37	8,470	1.6	0.50
B-38	9,795	1.0	0.90
B-39	10,150	1.1	0.92
B-20	10,500	1.1	0.67
B-21	11,010	1.3	0.67
B-40	11,180	1	0.90
B-22	11,210	1.1	0.78
B-30	14,060	1.3	0.67

Table 2. Summary of NMR Analyses of Mowry Formation, Wind River Basin Shales

Sample	Depth, ft	% TOC	Aromaticity
WR-14	2,480	1.3	0.5
WR-15	3,210	2.4	0.25
WR-1	4,100	--	0.58
WR-16	5,190	1.8	0.48
WR-3	6,900	--	nd
WR-18	7,720	1.9	0.38
WR-19	8,355	1.4	0.44
WR-5	8,960	--	nd
WR-20	9,090	2.2	0.55
WR-21	10,015	1.8	0.45
WR-7	10,350	--	>0.6
WR-10	12,440	--	>0.8
WR-22	12,715	2.3	0.44
WR-23	14,255	1.1	0.96
WR-11	14,280	--	>0.8

nd: not determined because of low TOC

Table 3. Summary of NMR Analyses of Denver Basin Samples

Sample	Location	Depth, ft	% TOC	Aromaticity
Mowry/Huntsman Formatiuon				
DM-15	2N-57W-29	4,840	2.2	0.45
DM-12	2N-57W-29	5,490	2.4	0.47
DM-9	2N-60W-33	6,500	2.2	0.51
DM-7	2N-62W-5	6,790-95	3.1	0.64
DM-6	2N-63W-19	7,370-75	1.5	0.58
DM-5	2N-64W-14	7,500-10	3.3	0.68
DM-4	2N-65W-6	7,820	1.8	0.94
DM-2	2N-67W-10	8,110	2.7	0.80
APX-8	--	1,580	2.1	0.60
APX-8	--	1,590	1.9	0.53
APX-8	--	1,608	1.4	0.57
D129	--	1,936	1.6	0.58

Sample	Well	Location	Depth, ft	Aromaticity
Niobrara Formation				
DN17	1-27 Brandon Cross	27-2N-50W	3110	nd
DN16	1 Pieper	17-2N-51W	3550	0.34
DN15	1 Wells	27-2N-52W	3690	0.50*
DN13	1 Hunt	8-2N-55W	4100	0.46*
DN14	1 Schmidt-B	26-2N-54W	4110	0.47*
DN12	1 Huey A	19--2N-56W	4200	nd
DN11	2 Marqardt	29-2N-57W	4730	0.37
DN10	4 Messenger	25-2N-58W	4910	0.39

Table 3. Summary of NMR Analyses of Denver Basin Samples, Cont.

Sample	Well	Location	Depth, ft	Aromaticity
Niobrara Formation				
DN9	1 B Funk	12-2N-59W	5220	0.40*
DN8	1 Epple	33-2N-60W	5700	nd
DN7	1 13State	13-2N-61W	5710	0.38
DN1	1 State B	16-2N-69W	6020	0.78*
DN6	1 Prospect Royalty	5-2N-62W	6230	0.52
DN5	1 Bergland	19-2N-63W	6720	0.70*
DN4	#2 Ivan Dale	14-2N-64W	6800	0.60*
DN2	1 Golden Turkey	10-2N-67W	7270	nd
DN3	1 C Pan Am -38	11-2N-66W	7340	0.66*

nd: not determined because of low TOC

* aromaticities are approximate because of low TOC's

Table 4. Summary of NMR Analyses of Alberta Basin Samples

Sample	Location	Depth, meters	Aromaticity	Remarks
Fish Scale Formation				
CH-B44	6-29-69-6	1,666	0.75	shale
CH-B73	10-3-72-12	1,726	0.71	shale
CH-B61	10-3-70-10	1,776	0.77	shale
CH-B70	11-15-70-11	1,819.3	0.82	coal
CH-B5	10-31-65-3	1,941	0.65	shale
CH-B65	10-3-70-10	1,950.1	0.70	shale
CH-B49	7-5-69-9	2,067.7	0.79	coal
CH -B11	10-35-65-5	2,106.5	0.75	coal
CH-B12	10-35-65-5	2,107	nd	shale
CH-B14	10-35-65-5	2,121	0.83	coal
CH-B36	10-31-68-10	2,151-2,160	0.79	coal
CH-B6	6-4-65-5	2,280	0.88	shale
CH-B10	6-4-65-3	2,298	0.76	coal
CH-B50	10-7-69-12	2,333	0.83	shale
CH-B52	10-7-69-12	2,341.5	0.87	coal
CH-B55	10-7-69-12	2,344	0.82	coal
CH-B40	7-1-68-12	2,430	0.81	shale
CH-B41	7-1-68-12	2,431	0.78	coal
CH-B21	6-32-65-7	2,545	0.80	coal
CH-B18	7-7-65-7	2,574.3	0.76	shale
CH-B32	10-19-66-9	2,580	0.82	shale
CH-B23	14-24-65-10	2,763	0.83	shale

Table 4. Summary of NMR Analyses of Alberta Basin Samples

Sample	Location	Depth, meters	Aromaticity	Remarks
Falher Formation	**Cuttings**			
CH-A32	7-25-68-7	1,935	0.75	coal
ALB5	11-4-70-11W6	1.965.5	0.71	coal
ALB9	7-20-69-10W6	2048	0.76	coal
CH-A29	10-33-67-7	2,290	0.78	coal
ALB7	8-2-66-9W6	2,570	0.86	coal
CH-A20	10-29-65-8	2,770	0.84	coal
CH-A9	9-9-64-8	2,980	0.84	coal
CH-A3	10-2-60-5	3,249	0.92	coal
CH-A5	10-13-62-9	3,445	0.88	coal

Table 5. Summary NMR Analyses of San Juan Basin Samples

Sample	Depth, ft	Aromaticity
Graneros Formation		
SV-1	1,000	nd
SV-2	2,000	nd
SH-19	2,160	0.42
SH-17	2,460	0.59
SH-16	3,750	0.59
SH-15	4,240	0.48
SH-14	4,770	0.62
SH-13	5,730	0.46
SV-3	3,040	0.69
SH-12	6,200	0.54
SH-9	6,430	0.61
SV-4	3,600	0.82
SV-7	6,370	0.91*
SH-2	6,700	0.91
SH-7	6,720	0.87
SH-4	7,380	0.95
SH-6	7,780	0.93
Menefee Formation		
SMC-11	1180	0.56
SMC-12	1400	0.57
SMC-10	2160	0.68
SMC-9	2350	0.60
SMC-8	3060	0.52
SMC-6	3710	0.62

Table 5. Summary NMR Analyses of San Juan Basin Samples, Cont.

Sample	Depth, ft	Aromaticity
SMC-7	4180	0.71
SMC-5	4380	0.66
SMC-2	4950	0.90
SMC-4	5000	0.85
SMC-3	5430	0.84
SMC-1	5640	0.79

* Aromaticity is approximate due to poor S/N ratio of NMR spectra

Table 6. Summary of Washakie Basin Data

Sample	Description	Depth, ft	Aromaticity	Remarks
MV21	Govt. C-38	3,000	0.82	
MV22	Playa Unit 5-24G	4,894	0.72	
MV1	AUPRR 44-35	4,560	0.72	shale
MV1B	AUPRR 44-35	4,560	0.69	coal
MV2	AUPRR 44-35	4,594	0.76	shale
MV3	Arch Unit 33B-12-4	4,688	0.73	shale
MV4	33B-12-4	4,694	0.83	shale
MV5	33B-12-4	4,721	0.75	shale
MV6	Playa Unit 5-24G	4,883.5	0.680	coal
MV7	Playa Unit 5-24G	4,894	0.67	coal
MV8	Arch Unit 14-24-4	4,900	0.62	shale
MV12	Table Rock 59	6,600	0.75	shale
MV13	Table Rock 59	6,665	0.74	shale
MV14	Table Rock 59	6,667	0.67	coal
MV15	Fed 44-4	6,789	0.71	shale
MV16	" "	6,861	0.72	shale
MV23	Bar Cross 63X-21	6,943.5	0.69	coal
MV9	Higgins 13A	7,013	0.69	
MV19	Higgins 13A	7,013	0.72	coal
MV24	Robinson Siding #1	7,441	0.71	shale
MV10	Blue GapII 2-8-14	9,055	0.77	shale
MV11	Blue GapII 7-4-92	9,150	0.72	coal
MV20	Enterprise A-1	10,663	0.84	
MV17	Celsius 16-1	12,265	0.88	shale
MV18	" "	12,273	0.87	shale
MV25	Champlin 535	13,543	0.88	
MV26	1 Champlin,	14,314	0.85	shale
MV27	5.G.U.3 coal	10,719.5	0.77	coal
MV28	" "	10,837	0.75	coal
MV29	Champlin 535	13,661	0.90	shale

Mario's Mesaverde Samples

Sample	Description	Depth, ft	Aromaticity	Remarks
MV30	Well B-103	4,693	0.69	Shale
MV31	Well B-103	4,884	0.75	Coal
MV32	Well A-222	9,150	0.78	Coal
MV33	Well A-222	9,159	0.75	Shale
MV34	Well A-904	10,898	0.83	Coal
MV35	Well A-904	10,946	0.83	Shale
MV36	Well B-088	12,071	0.78	Shale
MV37	Well B-191	12,091	0.80	Coal
MV38	Well B-088	12,121	0.79	Shale
MV39	Well D-493	12,604	0.94	Shale
MV48	Well Adobe	13,000	0.91	Coal
MV40	Well B-109	13,223	0.89	Shale
MV41	Well B-111	13,659	0.90	Shale
MV42	Well B-191	14,286	0.80	Coal
MV43	Well WW	14,929	0.80	Coal
MV44	Well WW	14,942	0.90	Shale
MV45	Well WW	16,119	nd	Shale
MV46	Well Koch. Mont.	17,330	0.94	Shale
MV47	Well Koch. Mont.	18,420	0.96	Shale
AL42	Champlin 529	3,378	0.75	shale
AL8	Champlin 242D1	4,358	0.71	coaly shale
AL4	Champlin 242D1	9,379	0.78	coaly shale
AL6	Champlin 242D1	9,394	0.76	coal
AL1	Champlin 242D1	9,420	0.77	coal
AL14	Champlin 242D1	9,388	0.92	shale
AL21	Champlin 242D1	9,618	0.68	coal
AL28	Champlin 242D1	9,298	0.79	coal
AL38	Champlin 242D1	9,497	0.81	shale
AL40	Champlin 446	14,273	>0.9	shale
1MV	mine		.841	coal
2MV	mine		0.92	coal
2AMV	mine		0.90	coal
3MV	mine		0.85	coal
5MV	mine		0.68	coal
MVHPO	Almond Coal		0.71	initial coal, hydrous pyrolysis

Mario's Mesaverde Samples

Sample	Well Name	Depth, ft	% Org. Carbon	Aromaticity	Remarks
PY8	1 USA Clark Oil & Ref.	4374	74.2	0.64	coal
PY9	1 USA Clark Oil & Ref.	4386	77.2	0.65	coal
PY10	1 USA Clark Oil & Ref.	4410	62.3	0.64	coal
PY11	1 USA Clark Oil & Ref.	4415	63.6	0.64	coal
PY18	6 Long Island Unit	4655	70.0	0.65	coal
PY15	4 Long Island Unit	4957	78.1	0.69	coal
PY16	4 Long Island Unit	4960	78.1	0.70	coal
PY17	4 Long Island Unit	4987	71.6	0.66	coal
PY12	5 Long Island Unit	5035	2.3	0.66	shale
PY13	5 Long Island Unit	5037	76.5	0.68	coal
PY14	5 Long Island Unit	5053	5.5	0.65	shale
PY6	63x-21 Bar Cross	6944	80.4	0.71	coal
PY7	63x-21 Bar Cross	6954	1.4	0.69*	shale
PY1	1 Old Road	8377	3.4	0.71	shale
PY2	1 Old Road	8384	1.3	0.72*	shale
PY3	1 Aspirin	8574	2.8	nd	shale
PY4	1 Aspirin	8582	0.9	0.85*	shale
PY5	1 Aspirin	8594	77.7	0.66	coal

nd: not determined

* Approximate value, poor quality spectra because of low TOC

Table 7. Summary of NMR Analysis of Minnelusa Formation, Powder River Basin

Sample	Well	Depth, ft	% TOC	Aromaticity
PM1	Robinson 1	5,805	1.3	0.78
PM2	Maey Gov't 1-30-1	7,125	1.7	0.73
PM3	P. Krause F22-31	7,970	1.5	0.74
PM4	Krause F21-3-P	8,345	1.3	0.70
PM5	Gov't 1-19	9,150	1.9	0.67
PM6	Superior-Raitt	10,097	1.4	0.75
PM7	Walters 7-30	11,035	1.1	0.72
PM8	Pre 27	11,360	1.1	0.76
PM9	Hunter Fee 21-30	12,010	1.1	0.75
PM10	Meijeh 1-35	14,550	1.1	0.74
PM11	Frye-1	14,565	1.1	0.74

NMR Measurements

NMR measurements were made using the technique of cross polarization (CP) with magic-angle spinning (MAS) on a Chemagnetics CMX solids NMR spectrometer. A large volume (~2.1 mL, 12.5 mm dia) NMR sample spinner was used to acquire NMR data on the Bighorn and Washakie Basin samples. ^{13}C NMR measurements were made at 25 MHz using a spinning rate of ~3.8 kHz. Because of the low levels of total organic carbon (TOC) in the Bighorn Basin samples (Table 1), 64,800 transients were recorded with a 1-s pulse delay. This corresponds to 18 hrs of signal averaging. Other instrument parameters were: contact time of 1 ms, pulse width of 6.2 μs , sweep width of 16 kHz, and 512 data points. A 50-Hz exponential multiplier was applied to the free induction decay of each ^{13}C spectrum before integration.

In the case of the Wind River Basin samples, there was not sufficient sample material to fill the large-volume sample spinner. Therefore, a small-volume (~0.5-mL) 7.5-mm pencil rotor was used. The samples were also washed with 6N HCl prior to making the NMR measurements. This procedure has been shown to provide some improvement in NMR sensitivity for materials containing low levels (~1%) of TOC. NMR spectra for the Wind River Basin samples were acquired at 50-MHz ^{13}C frequency, 1-s pulse delay, 1-ms contact time, 4.1-μs 90° pulse, 32-kHz sweep width, and 1 K data points.

Because of the low levels of organic carbon in the samples from the Bighorn and Wind River Basins, long-term signal averaging was employed to accumulate an NMR signal. However, the long-term averaging introduced background signals arising from some of the materials used in construction of the NMR probes. Usually background signals are not a factor when recording signals from samples containing high levels of carbon that yield signals in a shorter time, such as coals.

Background signals were recorded for the 12.5- and 7.5-mm probes under identical conditions as the source rock samples but using silica gel as a blank. The background signals were then digitally subtracted from the total signal. NMR integrations for the Bighorn and Wind River samples were performed on the spectra that were corrected for probe background signals.

NMR spectra of the samples from the Alberta, Denver, and San Juan Basins were obtained using a ceramic NMR probe that uses a 7.5-mm zirconia pencil rotor. The ceramic probe eliminates the background signal that arises from samples having low total organic carbon contents for which signal averaging over long periods of time is required. These spectra were obtained at a ^{13}C frequency of 25 MHz, a 90° pulse width of 5 μs, a contact time of 1 ms, and a pulse delay of 1 s. Signal averaging times ranged from 15 to 20 hrs per sample using this probe (54,000 to 72,000 transients) for samples having %TOC values of less than 2%. In some cases, NMR signals were not observed after long periods of signal averaging because of the almost nil TOC contents of the samples or because of severe line broadening resulting from paramagnetic materials in the samples.

Liquid-state ^{13}C NMR spectra of the hydrous pyrolysis oils were recorded using a 7.5-mm pencil rotor probe. Liquid spectra were recorded at a frequency of 25 MHz, at a pulse delay of 1 s, using a single pulse sequence with continuous decoupling. A few drops from a stock solution of chromium (III) acetylacetonate in $CDCl_3$ (0.1 molar) were added to shorten the relaxation times. The whole oil was placed in a glass tube with an outside diameter the same as that of the solid sample rotors. The sample tubes were then placed in the NMR probe and the signal recorded without spinning. Typically, 1800 transients were recorded to obtain the NMR spectra of the liquids.

For the carbon aromaticity measurements on the solid samples, the integrations covered the range from 340 to -80 ppm. This large range was required to include contributions to the aromatic carbon signals from spinning sidebands at ~300 and ~-40 ppm. For all the samples, the region between 340 and 90 ppm was considered the aromatic region. Any minor contributions from carbonyl and carboxyl carbons in the region between 210 and 165 ppm were also included in the aromatic component. The region between 90 and -20 ppm was considered the aliphatic carbon region. The integrated sideband intensity between -20 and -80 ppm was added to the aromatic carbon integral. The liquid-state NMR spectra were integrated from 0 to 60 ppm for the aliphatic carbons and 100 to 160 ppm for the aromatic carbons.

Because of the nature of the CP/MAS experiment, concerns about the accuracy of the carbon aromaticity measurements have been raised and have been debated (Snape et al. 1989). One concern is the use of a single contact time for determining carbon aromaticities. Aliphatic and aromatic carbons cross-polarize at different rates, and therefore a single contact may not give representative aromaticities. However, Wilson et al. (1991) compared aromaticities of coaly source rocks from the North Sea Brent Group obtained with a contact time of 1 ms, with aromaticities obtained by varying the contact time between 10 μs and 8 ms. The optimum signals from the aliphatic and aromatic carbons were obtained by curve-fitting the variable contact time data. In all but one case, the aromaticities at 1 ms contact time agreed with those from the variable contact time experiment within experimental error. They concluded that CP/MAS ^{13}C NMR measurements of the structure of sedimentary organic matter made at a 1-ms contact time (as used in this study) could be used with confidence.

Hydrous Pyrolysis Experiments

Hydrous pyrolysis experiments were conducted following the procedure of Lewan (1985). In these experiments, 200 g of coal was mixed with 400 g of distilled water and placed in a stainless steel reactor. The remaining space within the reactor was purged and left pressurized at 20 psi of helium. The coals were matured to different stages by heating separate samples of the same coal isothermally for 72 hrs at temperatures ranging from 290 to 360 °C. In some cases, the samples were heated for longer periods at 360 °C to achieve advanced stages of maturation.

Three organic phases were collected from the reactor after the hydrous pyrolysis experiment—an oil, a bitumen, and a coal residue or unreacted coal. The expelled oil occurred as a floating liquid pyrolysate layer on the water surface and as a sorbed liquid pyrolysate film on the coal surface. The floating liquid pyrolysate was collected and decanted into a separatory funnel where the pyrolysate was concentrated and collected. Hydrocarbons adhering to the reacted coal were washed with dichloromethane. In addition, the reactor walls and collection apparatus were also

washed with dichloromethane. The resulting solution was filtered and the pyrolysate concentrated by removing the solvent by rotary vacuum evaporation. The concentrated material was then allowed to dry in air to a constant weight. There were no significant differences between the floating material and the sorbed material, and collectively these materials are referred to as expelled oil. Typically, the floating material comprised more than 75% of the expelled oil.

Bitumen extractions were carried out on selected hydrous pyrolysis residues. The bitumen was extracted for 72 hr in a Soxhlet apparatus using a 60:40 mixture (by mass) of benzene and methanol. The refluxed solvent was filtered and the bitumen was recovered by rotary vacuum evaporation. Mass balance and NMR from the hydrous pyrolysis experiments are given in Table 8.

Anhydrous Pyrolysis Measurements

Anhydrous pyrolysis (Rock-Eval type pyrolysis) measurements were made on the drill cuttings to determine the thermal maturity of the sediments (Tissot and Welte 1984). In anhydrous pyrolysis, a small amount of sample is heated nonisothermally at a rate of 10 to 20 °C to a temperature of 550 °C. During heating, the free or adsorbed hydrocarbons are volatized at low temperature. This material is referred to as the S_1 or low-temperature peak. At higher temperature, pyrolysis of the kerogen produces hydrocarbon-like materials. This peak in the chromatogram is referred to as the S_2 peak. The production index (PI) is defined as the ratio of $S_1/(S_1 + S_2)$. This ratio is a measure of how much of the kerogen has been transformed to hydrocarbons as a result of thermal maturation.

Clay Diagenesis Measurements

X-ray diffraction measurements were made on the clay-sized fractions from the drill cuttings to monitor the transformation of smectite to illite as a function of burial depth. With increasing depth and consequently higher temperature, smectite releases bound water and becomes illite. This dehydration step has been used as an indicator of thermal maturation. X-ray diffraction measurements were made on a Scintag 2000 X-ray diffractometer. The method of Srodon (1980) was used to estimate the percentages of smectite and illite in the mixed-layer clays.

Other Analyses

The gases generated during hydrous pyrolysis were analyzed on a Varian 3760 gas chromatograph using a 30-ft-long, 1/8-in.-diameter Haysep DB column and thermal conductivity detection. Mono- and di-carboxylic acid anions in the waters were measured on a Dionex System

Table 8. Summary of Mass Balance and NMR Data for Almond and Lance Coals[a]

Temp., °C	Carbon in coal, g	Aliphatic carbon fraction, coal	Carbon in oil, g	Aliphatic carbon fraction, oil	Aliphatic carbon in gas, g	Aliphatic carbon in acid anions, g	Carbon in CO_2, g
Almond Coal							
20	139.2	0.29	0.00	0	0.00	0.00	0.00
290	133.2	0.28	0.82	0.83	0.21	0.67	1.25
300	131.9	0.27	1.24	0.83	0.31	0.60	1.62
310	130.4	0.22	2.05	0.86	0.46	0.78	2.03
320	122.2	0.22	2.51	0.87	0.69	1.07	2.49
330	122.7	0.18	3.25	0.85	1.01	1.21	2.68
340	123.3	0.19	4.01	0.85	1.45	1.33	2.85
345	122.3	0.17	4.57	0.81	1.70	1.39	2.59
350	121.2	0.17	4.44	0.77	1.93	1.50	2.58
360	121.3	0.14	3.61	0.80	2.70	1.16	2.83
Lance Coal							
20	138.4	0.30	0	0	0	0	0
290	133	0.21	0.84	0.8	0.23	0.46	2.17
300	135.8	0.17	1.23	0.8	0.36	0.54	2.51
310	127.7	0.19	1.83	0.84	0.52	0.61	2.69
320	128.5	0.14	2.19	0.84	0.81	0.77	3.03
330	124.2	0.15	3.4	0.81	1.08	0.78	3.26
340	122.4	0.17	4.21	0.77	1.53	0.77	3.57
345	124	0.15	3.75	0.83	1.83	0.86	2.97
350	123.5	0.13	3.85	0.81	2.12	0.68	3.1
360	120.1	0.12	3.97	0.72	2.63	0.73	4.68

[a] based on a 200-g sample of coal

12 chromatograph using the ion exclusion chromatography procedure described by MacGowan and Surdam (1994). Carbon values were determined using standard instrumental methods.

RESULTS AND DISCUSSION

Natural Maturation

Bighorn Basin

Geological Setting. The Bighorn Basin in northwestern Wyoming and southwestern Montana is both a structural and a topographic basin. The basin is bounded by the Owl Creek Mountains to the south, the Bighorn Mountains to the east, the Absoraka Volcanics to the west, and the Beartooth Mountains to the northwest. The basin is asymmetric with the axis of the deepest part of the sedimentary basin far to the west of the basin topographic center. In the Bighorn Basin, the Cretaceous sequence—the Lance, Mesaverde, Cody, Frontier, Mowry, and Thermopolis Formations—consists of 4,200 to 8,200 ft of shales, mudstones and sandstones that were deposited in nearshore, offshore, and fluvial environments during transgressions of the epicontinental seaway (Hagen 1986).

Overpressuring within the Cretaceous shale of the Bighorn Basin developed regionally in one large and continuous volume of rock. The onset of overpressuring is marked by a transitional pressure section approximately 3,000 ft thick. A hard overpressure section (overpressured more than 2,000 psi) underlies this transitional pressure section. The top of the transitional pressure section occurs at a depth of 9,000 ft ±1,000 ft, and the top of the hard overpressure section occurs at a depth of 12,000 ± 1,000 ft. Both tops are flat and are not restricted by stratigraphic boundaries (Jiao et al. 1993)

NMR measurements Previous studies have shown that NMR measurements provide important information on the diagenesis and maturation of the organic matter in shales and coals (Miknis et al. 1993). Basically, the NMR measurements show how the distribution of aliphatic and aromatic carbons changes with time and temperature during burial. The loss of aliphatic carbon is associated with oil and gas production because these carbons have a sufficient number of attached hydrogens to produce hydrocarbons (Patience et al. 1992, Miknis et al. 1993). Aromatic carbons, being hydrogen deficient, generate little oil or gas.

However, not all of the decrease in aliphatic carbons can be attributed to oil and gas formation. Some of the aliphatic carbon aromatizes during maturation, but the amount cannot be determined without mass balance measurements (Miknis, 1992b). Nevertheless, by monitoring the

aliphatic and aromatic carbons as a function of burial depth, limits can be placed on the capacity of source rocks to generate hydrocarbons. Such information is difficult, if not impossible, to obtain by other methods. The changes in the carbon aromaticities with depth for samples from the different sedimentary basins are given in Tables 1-7.

The CP/MAS ^{13}C NMR spectra of the Mowry shales from the Bighorn Basin as a function of present depth of burial are shown in Figure 2. A plot of the carbon aromaticity versus depth of burial is shown in Figure 3. The carbon aromaticities are fairly constant to a depth of ~8,500 ft. However, the spectra indicate that there is little capacity to generate hydrocarbons beyond a present-day burial depth of ~10,000 ft because little of the hydrogen-rich aliphatic component remains at this depth. These results are in general agreement with the previous NMR results for Mowry shale from the Powder River Basin (Miknis et al. 1993).

Other Maturation Measurements. The trend with depth of the production index (PI) shows a marked increase in the hydrocarbon production beyond a present-day depth of 9,000 ft (Figure 4). Above 9,000 ft the PI is typically less than or near 0.1. Below 9,000 ft the PI is greater and rises to 0.25 at 14,000 ft. These trends are in agreement with the aromaticity-vs-depth trend determined from the NMR data.

The above discussion implies that the organic material above ~9,000 ft matured in a different thermal regime than the material below 9,000 ft. This observation is strongly supported by the clay diagenetic trend shown in Figure 5. Illitization of smectite is largely completed at a present-day burial depth of 9,000 ft.

Wind River Basin

Geological Setting. The Wind River Basin, located in central Wyoming, (Figure 1) is one of many structural and sedimentary basins that formed in the Rocky Mountain foreland during the Laramide Orogeny (Keefer 1965). The basin is bounded by the Owl Creek and Bighorn Mountains to the north, the Casper Arch to the east, the Granite Mountains to the south, and the Wind River Range to the west. The basin is structurally asymmetric, with the deepest part of the sedimentary basin to the northeast, near the Owl Creek Mountains and Casper Arch. The Cretaceous strata in the Wind River Basin record a marine-dominated sedimentary sequence, culminating in the eastward withdrawal of the epicontinental seas from central Wyoming and the onset of the Laramide Orogeny. The maximum Cretaceous thickness is over 10,000 ft, and all the Cretaceous Formations produce hydrocarbons (Keefer and Johnson 1993).

NMR Measurements. CP/MAS ^{13}C NMR spectra of the Mowry samples from the Wind River Basin are shown in Figure 6. The carbon aromaticities versus depth are shown in Figure 7. These spectra show a fairly uniform carbon distribution with burial depth down to ~12,700 ft. There is a fairly abrupt loss of aliphatic carbons by the time a depth of 14,255 ft is achieved. The data suggest that these shales have a significant potential to generate hydrocarbons down to a present-day depth of 14,000 ft.

Other Maturation Measurements. The NMR data are supported by vitrinite reflectance and anhydrous pyrolysis measurements. Vitrinite reflectance (R_o) values range from 0.55% at a depth of 4,100 to 2.5% at a depth of 18,300 ft (Jiao et al. 1993). A plot of the vitrinite reflectance versus depth is shown in Figure 8. Liquid generation is thought to occur between 0.5–0.7% and 1.0–1.3% R_o. Between 1.3 and 2.0% R_o, oil is thought to thermally crack to wet gas. As seen in Figure 8, there is a steep increase in the R_o value below 14,000 ft. The anhydrous pyrolysis measurements show low production indices down to 14,000 ft. These data are in agreement with the changes in aromaticity measured by NMR. The depth of the hard overpressure section occurs at 14,000 ± 1,000 ft and appears to result mainly from the liquid oil-to-gas reaction. Thus, the onset of overpressuring appears to be related to marked changes in the thermal maturation of the source rock.

Denver Basin

Geological Setting. The Denver Basin of Colorado, Wyoming, and Nebraska (Figure 1) is one of the major petroliferous basins in the Rocky Mountain area. It is bounded by the Chadron Arch on the northeast, the Las Animas Arch on the southeast, and the front range of the Rocky Mountains on the west. The basin is a structural syncline formed during the Laramide Orogeny. The interior basin is asymmetric, with a broad, gentle slope on the east flank and a steep dip on the west flank. The deepest part, located between Denver, Colorado, and Cheyenne, Wyoming, is called the Deep Basin. The basin axis is close to the front range. There are numerous lithic faults trending southwest-northeast in the basin. Vertically, the faults extend from the basement or lower Cretaceous to the middle Pierre shale of the upper Cretaceous and have short displacement (Sonnenberg 1987). Sediments range from Cambrian through Tertiary. The thick Cretaceous section is composed mainly of deltaic and marine detrital units and is the source of most of the Denver Basin oil and gas production. The source rocks in the Denver Basin are mainly shales in the Lower Cretaceous Skull Creek to the Upper Cretaceous Niobrara formations in the central basin area.

Sonic and resistivity logs have been used to detect pressure anomalies in the Denver Basin. All logs were selected along an east-west cross section within Townships 1 and 2 north and Ranges 47 to 69 west. Pressure compartmentalization in the Denver Basin has been described by Jiao et al. (1994).

NMR Measurements. Samples from the Mowry/Huntsman and Niobrara Formation shales were analyzed by solid-state ^{13}C NMR. Representative NMR spectra of the Mowry/Huntsman and Niobrara Formation shales are shown in Figures 9 and 10, respectively. The carbon aromaticities versus depth are shown in Figure 11 for the Mowry/Huntsman shales. Down to a depth of 6,500 ft, the aromaticity increases slowly, while deeper than 6,500 ft, the aromaticity increases rapidly. At a present burial depth of ~7,800 ft there appears to be little capacity to generate additional hydrocarbons because of the small aliphatic carbon component in the rocks. These data support data obtained from velocity and resistivity logs on the eastern end of the basin between Ranges 60 and 61W (Jiao et al. 1994).

Other Maturation Measurements. Production indexes (PI) were determined on samples of the Mowry/Huntsman shales using hydrous pyrolysis (Figure 12). At depths shallower than 4,500 ft the PI is about 0.025. Between 4,500 and 6,500 ft the PI changes slowly from 0.025 to 0.05 then increases rapidly to 0.25 at a depth of 8,000 ft. The general trend of the production index data is similar to that of the carbon aromaticity data.

Samples of cuttings from the Mowry/Huntsman shales were analyzed by X-ray diffraction to determine the illite/smectite (I/S) content in the clays. The percentage of illite in the illite/smectite mixed-layer clay as a function of depth is shown in Figure 13. At a depth of about 6,500 ft there is a significant change in the illite percentage, from 20% to 75%, indicating a transformation of random to ordered I/S mixed-layered clays. This pattern is also in agreement with the other maturational indicators.

Alberta Basin

Geologic Setting. The Alberta Deep Basin in western Canada is located east of the tectonically disturbed belt of the Rocky Mountains in the provinces of Alberta and British Columbia (Fig. 1). It represents the deepest part of the huge, asymmetric Western Canada Basin. The Deep Basin is approximately 400 miles long and reaches a width of about 80 miles. A broad wedge of Paleozoic and Mesozoic sedimentary rocks trends northwesterly, thinning eastward to zero on the Canadian shield and thickening westward into the Rocky Mountains. Subsidence of the basin ended with the conclusion of the Laramide orogeny. The Mesozoic sequence consists largely of Cretaceous dark shales interlayered with sandstones and conglomerates. Coal seams are frequent, particularly in the deeper part of the Lower Cretaceous. Gas occurs in only the deepest part of the basin, at a depth greater than 1000 m. The lower Cretaceous has only recently been recognized as the foremost oil and gas source reservoir in Canada and, in fact, may be the richest in hydrocarbons of any group of rocks in the world (Masters 1984).

The Western Canada Basin contains outstanding examples of anomalously underpressured rocks, which are easily detected and delineated from sonic logs (Jiao et al. 1996). In the vicinity of the Elmworth gas field, this occurs at a depth of approximately 6,200 ft. In Laramide basins, such as the Powder River, Bighorn, Wind River, and Greater Green River Basins of Wyoming, the reversal in sonic travel time correlates well with the boundary between normally pressured and overpressured rocks. Whether the rock interface is under- or overpressured, the sonic log trends and patterns are the same.

A pattern of underpressured rock overlain by overpressured rock has been noted in the Laramide basins of Wyoming and Colorado. This pattern is particularly noticeable in those portions that have undergone maximum uplift and erosion. Underpressurized hydrocarbon accumulations are associated with regions that have experienced significant uplift and erosion. In the Powder River and Washakie Basins this varies from 1,000 to 2,000 ft in the basin centers and to more than 5,000 ft along the basin margins. By comparing depth trends with maturation parameters, Jiao et al. (1996) have shown that about 3,000 ft of uplift should be added to the Elmsworth area to match trends observed in the Powder River and Washakie Basins.

NMR Measurements. CP/MAS ^{13}C NMR spectra of the coal samples from the Fourth coal in the Alberta Basin are shown in Figure 14. Even though the coals have a significant aromatic carbon distribution, there is still an overall decrease in the aliphatic carbon fraction as a function of depth. In addition, the chemical shift maximum of the aliphatic carbons changes with depth, suggesting that the aliphatic carbons remaining at depth are probably due to methyl groups attached to aromatic rings. This is discussed in greater detail later in the section on artificial maturation.

Plots of the carbon aromaticities versus depth for samples of the Fourth coal and Fish Scale Zone of the Alberta Basin are shown in Figures 15 and 16, respectively. Data from the Washakie Basin are plotted for reference. When a 3,000-ft uplift correction is applied, the data from the Alberta Basin nicely follows the trend of the Washakie Basin.

Other Maturation Measurements. The trends with depth of the carbon aromaticity are similar to those obtained from other geochemical measurements of maturation. The trends with depth of the % illite in the mixed-layer illite/smectite clay, vitrinite reflectance, and production index are shown in Figures 17-19, respectively. In all cases, when a 3000-ft uplift correction is applied to the Alberta Basin samples, the trends nicely follow the trends with depth of the Washakie Basin samples. These data led to the conclusion that the Elmsworth area of the Alberta Basin experienced ~3000 ft more uplift than the central part of the Powder River or Washakie Basins and that ~5000 ft of uplift and erosion is needed to get significant underpressuring in Laramide Basins (Jiao et al. 1996).

San Juan Basin

Geological Setting. The San Juan Basin covers northwestern New Mexico and southwestern Colorado (Figure 1). The basin is bounded on the north by the San Juan uplift, on the east by the Nacimiento uplift, on the south by the Zuni uplift and on the west by the Defiance uplift and Four Corners platform. The basin has an irregular outline and can be divided into two main structural elements, the central and outer basins. The central basin is nearly circular in plan, but is strongly asymmetric in cross section, with a gently dipping southwestern flank and very steep flanks on all sides, especially the northern flank. The shape of the basin is remarkably smooth, with little or no modification by faulting or folding, except in the Colorado portion.

The sediments in the San Juan Basin are as much as 14,000 ft thick and range in age from Cambrian to Quaternary. Oil and gas production comes from Pennsylvanian, Jurassic, and, most important, from Cretaceous rocks. The hydrocarbon was generated from the Mancos shale, Menefee shale and coal, Lewis shale, and Fruitland coalbed in the northern Deep Basin.

NMR Measurements. CP/MAS ^{13}C NMR spectra were acquired on 10 shale cuttings from the Graneros shale and 11 coal and coaly shale samples from the Menefee shale in the Mesaverde Group. Representative spectra are shown in Figures 20 and 21. A plot of the carbon aromaticity with depth is shown in Figures 22 and 23. For the Graneros shale, there is a marked increase in the aromaticity from about 0.6 to 0.9 at a depth of 6500 feet. For samples from the Menefee shale, the aromaticity increases from 0.6 to 0.9 at a depth of about 4500 ft. The Menefee shale is about 2000 ft shallower than the Graneros shale. The maturation zone delineated by the Menefee shale is still coincident with the sonic anomaly zone (Zhao 1996).

Other Maturation Measurements. Vitrinite reflectance measurements were made on 14 samples of shale cuttings from the Graneros shale (Figure 24). R_0 reaches a value of 0.8%, the onset of gas generation, at a depth of 6500 ft. Similarly, the production index exhibits an abrupt change from 0.1 to 0.7 at about 6500 ft (Figure 25), and the percentage of illite in the illite/smectite mixed-layer clay undergoes an abrupt change between 6000 and 7000 ft (Figure 26). These measurements are all in agreement and delineate the maturation zone in the sonic velocity measurements (Zhao 1996).

Artificial Maturation

NMR Characterization of Hydrous Pyrolysis Residues

The CP/MAS ^{13}C NMR spectra for Almond and Lance coal hydrous pyrolysis residues are shown in Figures 27 and 28. The spectra clearly show a decrease in the aliphatic carbon fraction

relative to the aromatic carbons with increasing temperature. Aliphatic carbon structures are hydrogen-rich and are largely responsible for the oils and the hydrocarbon gases that are generated during natural and artificial maturation. The NMR spectra suggest that most of the oil is generated in the temperature range 290–330 °C because of the greater reduction in aliphatic carbon fraction relative to that of the starting materials in this temperature range.

The aliphatic carbon region shows partial resolution of at least two types of carbons. These have been assigned to methylene carbons (CH_2) in long chains (30 ppm), and methyl groups (CH_3) attached to aromatic rings (~20 ppm). Methylene carbons in branched and cyclic aliphatic structures are also counted with the methylene carbons at 30 ppm. The resolution is more noticeable at temperatures of 330 °C and higher. Spectra of residues generated at these temperatures show a shift in position of the maximum from 30 ppm to that of the CH_3 on aromatic rings at ~20 ppm. Methyl groups attached to aromatic rings would not be cleaved at these temperatures but would produce gas at higher temperatures.

There is a narrowing of the aromatic resonance band with increasing temperature. This narrowing is indicative of an increase in the number of fused rings in the polynuclear aromatic moiety and of a lesser amount of substitution on the aromatic rings as alkyl side chains are cleaved during oil and gas generation. During hydrous pyrolysis, cleavage of substituents bridging aromatic rings could initiate condensation reactions that yield larger aromatic cluster sizes. Aromatization of aliphatic carbons to produce larger, more condensed aromatic ring structures would limit the number of substituents per aromatic carbon in the ring. The net effect of all these changes is to narrow the chemical shift dispersion, which manifests itself as a narrowing of the resonance band. The general features of the NMR spectra for the hydrous pyrolysis residues as a function of temperature are similar to those observed for maturation of petroleum source rocks (Requejo et al. 1992) and coals as a function of rank (Miknis et al. 1981).

The CP/MAS ^{13}C NMR spectra also show a resonance band at ~180 ppm, which is attributed to carbons in a carboxylate functionality. During heating, decarboxylation reactions of these functional groups liberate CO_2. The CP/MAS ^{13}C NMR spectra in Figure 27 and 28 show that this carbon functionality disappears by the time a temperature of 300 °C is reached, illustrating rapid evolution of CO_2 during hydrous pyrolysis of subbituminous coals. During pyrolysis, rapid evolution of CO_2 is observed and is thought to be a major contributor to crosslinking and retrograde reactions (Solomon et al. 1990).

Residues of Lance coal from hydrous pyrolysis at lower temperatures were also available for NMR analysis so that the temperature range could be extended to lower temperatures. The change in the aliphatic carbon fraction as a function of temperature for the Lance coals is shown in Figure 29. The data show that there is little change in the carbon structure up to temperatures of 250 °C.

At temperatures greater than 250 °C there is a noticeable change in the aliphatic carbon fraction, which is indicative of devolatilization and aromatization reactions. Similar behavior has been observed during ballistic heating of Eagle Butte subbituminous coal from Wyoming. That is, heating to 250 °C produced little changes in the carbon structure; however, heating to 300 °C produced significant changes that were due to devolatilization and aromatization (Miknis et al. 1996).

Aromatization of Aliphatic Carbon During Hydrous Pyrolysis

Not all of the decrease in aliphatic carbons during maturation can be attributed to oil and gas formation. Some of the aliphatic carbon structures aromatize during maturation, but the amount cannot be determined without mass balance measurements (Miknis 1992, Miknis et al. 1996). Mass balance and elemental analysis data were available from hydrous pyrolysis experiments to determine the extent of aromatization of aliphatic carbon moieties during artificial maturation (Miknis et al. 1996). Carbon mass balance and NMR data for the hydrous pyrolysis of Almond and Lance coals are summarized in Table 8. The data are given on the basis of a 200-g sample of coal. The masses of aliphatic carbon in the coal and oil at each temperature are obtained by multiplying the masses of carbon in the coal and oil by their respective aliphatic carbon fractions. In this study, the %C was not obtained on the oil samples. Consequently, the carbon content of the oil was assumed to be 84% for the purposes of calculation. The results are not greatly affected by this assumption because the amount of liquid products generated was low. The major form of carbon in the gas was CO_2 (Table 8).

Some carboxylic acid anions (C_1 to C_4) were present in the water. The aliphatic components in these acids were assumed to originate from the aliphatic components in the original coal and were thus taken into account in the aliphatic carbon balances.

The number of aliphatic carbons that aromatize (C_a^{al}) is obtained by subtracting the total aliphatic carbon in the products (C_{al}^P) from the aliphatic carbon in the starting material (C_{al}^0),

$$C_a^{al} = C_{al}^0 - \sum C_{al}^P \quad (1)$$

However, because the aromatic carbon in the products can originate from either aromatic or aliphatic carbons in the starting coal, there is no way to partition the aliphatic carbon that aromatizes between the oil and residue.

The Almond and Lance coal carbon conversion data from hydrolysis pyrolysis have been compared to carbon conversion data from pyrolysis of a Colorado and a Kentucky oil shale and a

Wyodak subbituminous and an Illinois No. 6 bituminous coal (Table 9 and Figure 30). The pyrolysis data were obtained during isothermal pyrolysis experiments conducted at 425 °C for two hrs in a fluidized sandbath reactor. A number of features in Figure 30 are worth noting. The greater the number of aliphatic carbons in the starting material, the greater the total carbon conversion to liquids and gases. Also, the greater the number of aliphatic carbons in the starting material, the fewer the number of aliphatic carbons that aromatize. During oil and gas generation, free radicals that are formed by cracking reactions are capped by hydrogen atoms from the aliphatic carbon moieties. Removal of these hydrogens converts some of the aliphatic carbon to aromatic carbon.

In the absence of a hydrogen donor, the oil shale or coal must donate its own hydrogen to form stable hydrocarbon liquids and gases. Thus, the carbon structure of the starting material is of major importance. For Colorado oil shale, the produced liquids are generally quite aliphatic so that fewer hydrogen atoms per carbon removed are needed to cap the radicals and form stable products when the long chain alkyl constituents are cleaved from the aromatic rings. In this case, hydrogen utilization is efficient. Only about 5 of 74 carbons were needed to cause a 79% conversion of carbon to volatile products.

In the case of coals, the alkyl side chains are short, as are the bridges between rings. The opportunity to form long chain paraffinic products is not great. Instead, more hydrogen atoms per carbon are required to cap off radicals and to remove a smaller number of carbon atoms as gas and liquid products. The net effect is an inefficient use of hydrogen that results in a significant fraction of aliphatic carbons that aromatize.

NMR Spectra of Washakie Basin Coals and Shales

The CP/MAS ^{13}C NMR spectra of Almond Formation coals and shales from the Washakie Basin as a function of burial depth exhibit changes similar to those observed during hydrous pyrolysis. Representative spectra are shown in Figures 31 and 32. During hydrous pyrolysis, the average carbon aromaticity of the Lance and Almond coals increased from 0.75 to 0.87 between 290 and 360 °C. Some oil and gases are also produced over this temperature interval. In the natural environment, corresponding changes in the carbon aromaticity are observed for burial depths of ~9,000 to ~15,000 ft. The oil generation window in the center of the Washakie Basin is thought to be from ~4,000 to ~12,000 ft. At greater depths cracking of oil to gas is thought to occur. The changes in carbon aromaticity observed during hydrous pyrolysis and natural maturation are consistent with these interpretations. However, because the samples were obtained from different areas of the Washakie Basin, the burial history for each sample may be different. Therefore, strict correlations between level of maturation and present depth of burial are not expected for all samples.

Table 9. Summary of Carbon Aromatization During Pyrolysis and Hydrous Pyrolysis

	Temperature, °C	Time, hrs	Number of Carbons Converted	Number of Original Aromatic Carbons	Number of Original Aliphatic Carbons	Number of Aliphatic Carbons Aromatized
Pyrolysis						
Colorado oil shale	425	2	78.80	25.60	74.40	4.60
Kentucky oil shale	425	2	46.00	49.00	51.00	9.60
WyoDak coal	425	2	17.90	61.10	38.90	15.10
Illinois #6 coal	425	2	17.00	68.00	32.00	11.52
Hydrous Pyrolysis						
Almond coal	360	72	12.90	71.30	28.70	11.73
Lance coal	360	72	13.20	70.40	29.60	14.95

Aromatic Ring Cluster Size

Exploratory NMR measurements were made to obtain information about the increase in the number of fused rings in the polynuclear aromatic moieties during natural and artificial maturation. In this procedure, dipolar dephasing NMR measurements were made to determine the number of aromatic carbons that have attached hydrogen atoms (Murphy et al. 1982). Additional structural parameters were obtained from integration of different regions of the CP/MAS spectrum. These data were then used to derive a number of parameters related to the carbon skeletal structure (Solum et al. 1989).

One carbon skeletal parameter of interest in maturational studies is the average size of the aromatic carbon cluster. The dipolar dephasing NMR procedure was used in conjunction with normal CP/MAS NMR measurements to obtain estimates of the changes in the size of the aromatic clusters with depth for San Juan Basin samples and with temperature during hydrous pyrolysis for Lance coal samples (Table 10). The results indicate that the aromatic clusters in the naturally and artificially matured samples consist of about four fused rings, whereas the immature San Juan Basin sample and the initial Lance coal before hydrous pyrolysis had an average cluster size of about two rings. These are the results that what would be expected during maturation; however, the NMR procedure provides a way to quantify the results.

Table 10. Aromatic Carbon Cluster Size of Naturally and Artificially Matured Coals

Sample	Burial Depth/ Temperature	Aromatic Carbons per Cluster
Natural Maturation		
San Juan Basin		
Menefee Fm.		
SMC-9	2,350 ft	8.4
SMC-2	4,950 ft	18.5
Hydrous Pyrolysis		
Washakie basin		
Lance Fm.		
LC0	initial	12
LC360	360°C	18

SUMMARY AND CONCLUSIONS

The main thrust of the research conducted during the contract period was to provide solid-state ^{13}C NMR measurements and interpretation in support of the various projects concerned with the multidisciplinary analysis of pressure compartments in different sedimentary basins. A summary of the samples and basins for which NMR measurements were made is given in Table 11 along with the ranges of TOC and depths of burial. The NMR data base generated during this project is unique. There have been no other studies reported in which NMR analyses have been made on as many samples from as many different sedimentary basins, burial depths, and TOC values as reported here.

Table 11. Distribution of Samples from Different Sedimentary Basins Analyzed by NMR

Basin	Formation	Number of Samples	Range in depth, ft	Range of %TOC
Alberta	Fish Scale/Harmon	31	1965 -11,300	~1.0 - 80.0
Bighorn	Mowry	16	1,100 - 14,060	0.7 - 2.0
Wind River	Mowry	16	2,480 - 14,280	1.1 - 2.4
Powder River[a]	Mowry	24	3,000 - 12,000	1.0 - 4.2
Powder River	Minnelusa	11	5,805 - 14,565	1.1 - 1.9
Denver	Mowry/Huntsman	12	1,580 - 8,110	1.4 - 3.3
Denver	Niobrara	17	3,110 - 7,340	nd
San Juan	Menefee/Graneros	29	1,000 - 7,780	nd
Washakie[b]	Lance/Almond	82	3,000 - 18,420	0.9 - 80.4

[a]Data acquired during previous contract, see Miknis 1992a
[b]Some data were aquired under different contract, see Miknis and MacGowan 1993
nd: not determined

The main benefit of the NMR measurements is that NMR provides a direct measurement of the organic carbon distribution in source rocks. This information is obtained in the form of a spectrum that is easy to interpret in terms of the source rock's capacity to generate hydrocarbons during maturation. These data can be used to place limits on the burial depths at which hydrocarbons are generated. In addition, when NMR is used in combination with laboratory experiments, insight into some of the chemistry of hydrocarbon generation can be gained.

In the Bighorn Basin, little aliphatic carbon remained in the rock sample beyond a present-day depth of burial of ~9,000 ft, indicating a change in the fundamental rock properties at this depth. In the Wind River Basin, the aliphatic carbon components disappeared at a present-day depth of 10,000 ft. In the Denver Basin, the aliphatic carbon disappeared at a depth of 7,800 ft. In the San Juan Basin, this occurred at ~6,500 ft in the Graneros shale and at ~4,500 ft in the Menefee shale. For shale samples from the Washakie Basin, little aliphatic component remained after ~12,000 ft, suggesting little additional capacity for oil generation at greater depths. Similar trends were noted for the coal samples; however, at the maximum depth sampled (10,837 ft), the coals still have some capacity for hydrocarbon generation. The maturation trends in the Alberta Basin nicely followed the depth trends in the Washakie Basin when a 3,000-ft. uplift correction was applied to the Alberta Basin data.

Solid-state NMR measurements on residues from hydrous pyrolysis of Almond and Lance Formation coals clearly showed a preferential loss of aliphatic carbons relative to aromatic carbons during heating. The amount of aliphatic carbon in the products was not sufficient to account for the total amount of aliphatic carbon that had disappeared. Between 40 and 50% of the aliphatic carbon aromatized during hydrous pyrolysis. The aliphatic carbon remaining in the residue appeared to be due to methyl groups attached to aromatic rings. In addition, there was a definite line narrowing in the aromatic carbon region, with increasing temperature due to cleavage of phenolic carbons and alkyl substituents during hydrocarbon generation. Rapid evolution of CO_2 also occurred during hydrous pyrolysis, as evidenced by the loss of carboxylate functionality in the NMR spectra at 300 °C.

There appears to be a direct relationship between thermal maturation and overpressuring. This relationship is reflected by various measurements of the organic geochemistry of the source rock related to thermal maturation, oil generation, and expulsion, and by changes in the level of clay diagenesis in the shales. These changes coincide with the onset of overpressuring.

REFERENCES

Hagen E.S., 1986, Hydrocarbon Maturation in Laramide-Style Basins: Constraints From the Northern Bighorn Basin, Wyoming and Montana, Ph.D. Dissertation, University of Wyoming, Laramie, 215 pp.

Jiao Z.S., R.C. Surdam, and F.P. Miknis, 1993, The Regional Pressure Regimes in the Cretaceous Shales in the Bighorn, and Wind River Basins, Wyoming, Ch. 5, *Gas Research Institute Annual Report*, GRI contract GRI 5089-260-1894, December 1993.

Jiao Z.S., H.Q. Zhao, and R.C. Surdam, 1994, Pressure Compartmentalization in Cretaceous Shales and Sandstones in the Washakie and Denver Basins, Ch. 3, *Gas Research Institute Annual Report*, GRI contract GRI 5089-260-1894, December 1994.

Jiao Z.S., R.C. Surdam, and F.P. Miknis, 1996, The Pressure Regime in the Vicinity of the Elmworth Area, Western Canada Basin Ch. 5, *Gas Research Institute Annual Report*, GRI contract GRI 5089-260-1894.

Keefer W.R., 1965, Stratigraphy and Geologic History of the Uppermost Cretaceous, Paleocene and Lower Eocene Rocks in the Wind River Basin, Wyoming, U.S. Geological Survey Professional Paper 495-A, 77p.

Keefer W.R. and R.C. Johnson, 1993, Stratigraphy and Oil and Gas Resources in Uppermost Cretaceous and Paleocene Rocks, Wind River Basin ,Wyoming in W. Keefer, W. Metzger, and L. Godwin, eds., Oil and Gas and Other Resources of the Wind River Basin , Wyoming: Special Symposium, Wyoming Geological Association, 71-86.

Lewan, M.D., 1985, Evaluation of Petroleum Generation by Hydrous Pyrolysis Experiments. *Phil. Trans. Royal So.* 315A: 121-134.

MacGowan, D.B., and R.C. Surdam, 1994, Techniques and Problems in Sampling and Analyzing Formation Waters for Carboxylic Acids and Anions, in *Carboxylic Acids in Sedimentary Basins*, E. Pittman and M. Lewan, eds., Springer-Verlag, New York, pp 22-39.

MacGowan, D.B., Z.S. Jiao, R.C. Surdam, and F.P. Miknis, 1994, Formation Water Chemistry of the Muddy Sandstone and Organic Geochemistry of the Mowry Shale, Powder River Basin, Wyoming: Evidence for Mechanism of Pressure Compartment Formation, *AAPG Memoir,* 61, P.J. Oroleva and Z. Al-Shaeib, eds., AAPG, Tulsa, OK, 321-332.

Masters, J.A., 1984, Lower Cretaceous Oil and Gas in Western Canada, *AAPG Memoir 38*, J.A. Masters ed, AAPG., Tulsa, OK, 1984

Miknis, F.P., M.J. Sullivan, V.J. Bartuska, and G.E. Maciel, 1981, Cross Polarization Magic-Angle Spinning ^{13}C NMR Spectra of Coals of Varying Rank. *J. Org. Geochem.*, 3, 19-28.

Miknis F.P. 1992a, Solid-State NMR Characterization of Mowry Shales, Western Research Institute, Laramie, WY, April 1992, WRI Report WRI-92-R025

Miknis, F.P., 1992b, Combined NMR and Fischer Assay Study of Oil Shale Conversion, *Fuel*, 71, 731-738.

Miknis F.P. and D.B. MacGowan, 1993, Solid-State NMR Analysis of Coals and Oil Shales from the Mesaverde Group, Greater Green River Basin, Wyoming, Laramie, WY, DOE report, DOE/MC/11076-3554.

Miknis, F.P., Z-S Jiao, D.B. MacGowan, and R.C. Surdam, 1993, Solid-State NMR Characterization of Mowry Shale From the Powder River Basin, *J. Org. Geochem.*, 20, 339-347.

Miknis F.P., D.A. Netzel, and R.C. Surdam, 1996, NMR Determination of Carbon Aromatization During Hydrous Pyrolysis of Coals From the Mesaverde Group, Greater Green River Basin, *Energy and Fuels*, 10, 3-9.

Murphy, P. D., T. J. Cassady and B. C. Gerstein, Determination of Apparent Ratios of Quaternary to Tertiary Aromatic Carbon Atoms in Anthracite Coal by ^{13}C -^{1}H Dipolar Dephasing NMR, *Fuel*, 1982, 61, 1233.

Patience, R.L., A.L. Mann, and I.J.F. Poplett, 1992, Quantitative Determination of Molecular Structure of Kerogens Using ^{13}C NMR Spectroscopy: The Effects of Thermal Maturation of Kerogens From Marine Sediments, *Geochim. Cosmochim. Acta*, 56, 2725- 2742.

Requejo, A.G., N.R. Gray, H. Freund, H. Thomann, M.T. Melchoir, L.A. Gebhard, M. Bernardo, C.F. Pictroski, and C.S. Hsu, 1992, Maturation of Petroleum Source Rocks. 1. Changes in Kerogen Structure and Composition Associated With Hydrocarbon Generation, *Energy and Fuels*, 6, 203-214.

Snape, C.E., D.E. Axelson, R.E. Botto, J.J. Delpeuch, P. Tekely, B.C. Gerstein, M. Pruski, G.E. Maciel, and M.A. Wilson, 1989, Quantitative Reliability of Aromaticity and Related Measurements on Coals by ^{13}C NMR. A Debate. *Fuel*, 68: 547-560.

Solum, M. S., R. J. Pugmire and D. M. Grant, ^{13}C Solid-State NMR of Argonne Premium Coals *Energy and Fuels*, 1989, 3, 187.

Solomon P.R., M.A. Serio, G.V. Despande,and E. Kroo, 1990, Cross-Linking Reactions During Coal Conversion, *Energy and Fuels*, 4, 42-54

Sonnenberg, S.A., 1987, Tectonic Sedimentary and Seismic Models for D Sandstone, Zenith Field Area, Denver Basin, Colorado, *AAPG Bulletin*, 71, 1366-1377.

Srodon, J., 1980, Precise Identification of Illite/Smectite Interstratifications by X-ray Powder Diffraction, *Clays and Minerals*, 28, 401- 411.

Tissot, B.P. and D.H. Welte, 1984, *Petroleum Formation and Occurrence*, 2nd Edition, Springer-Verlag, Berlin, 699 p.

Welte D.H., R.G. Schaefer, W. Stoessinger, and M. Radke, 1984, Gas Generation and Migration in the Deep Basin of Western Canada, *AAPG Memoir 38*, J.A. Masters ed, AAPG, Tulsa, OK, 1984

Wilson, M.A., A. Vassallo, D. Gizachew, and E. Lafargue, 1991, A High Resolution Solid State Nuclear Magnetic Resonance Study of Some Coal Source Rocks from the Brent Group (North Sea). *J. Org. Geochem.*, 17: 107-111.

Zhao, H., 1996, Anomalous Pressures in the Cretaceous Sandstones of the Denver and San Juan Basins (Rocky Mountain Laramide Basins), Ph. D. thesis, Department of Geology, University of Wyoming.

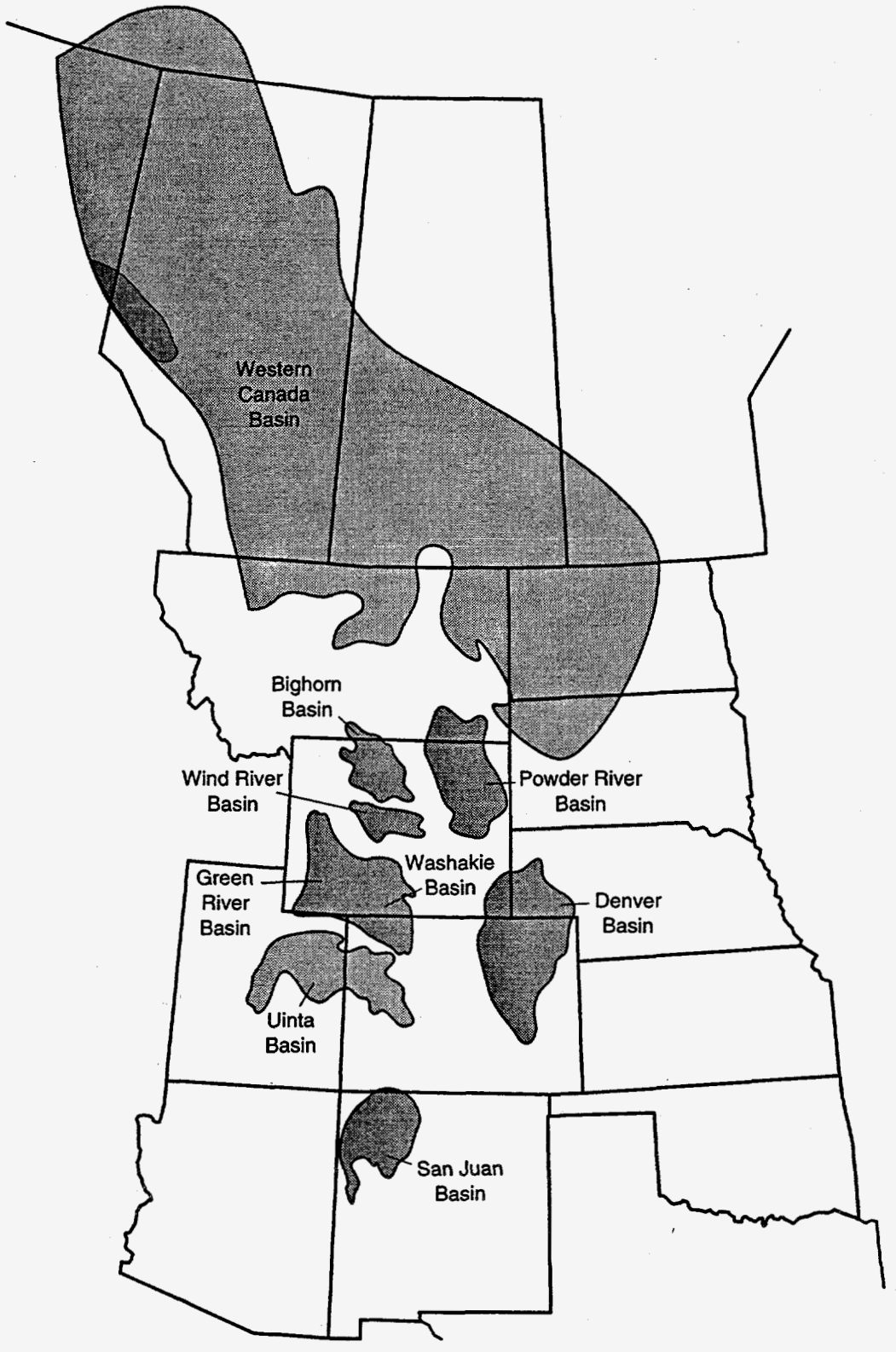

Figure 1. Map showing the major gas producing basins of North America

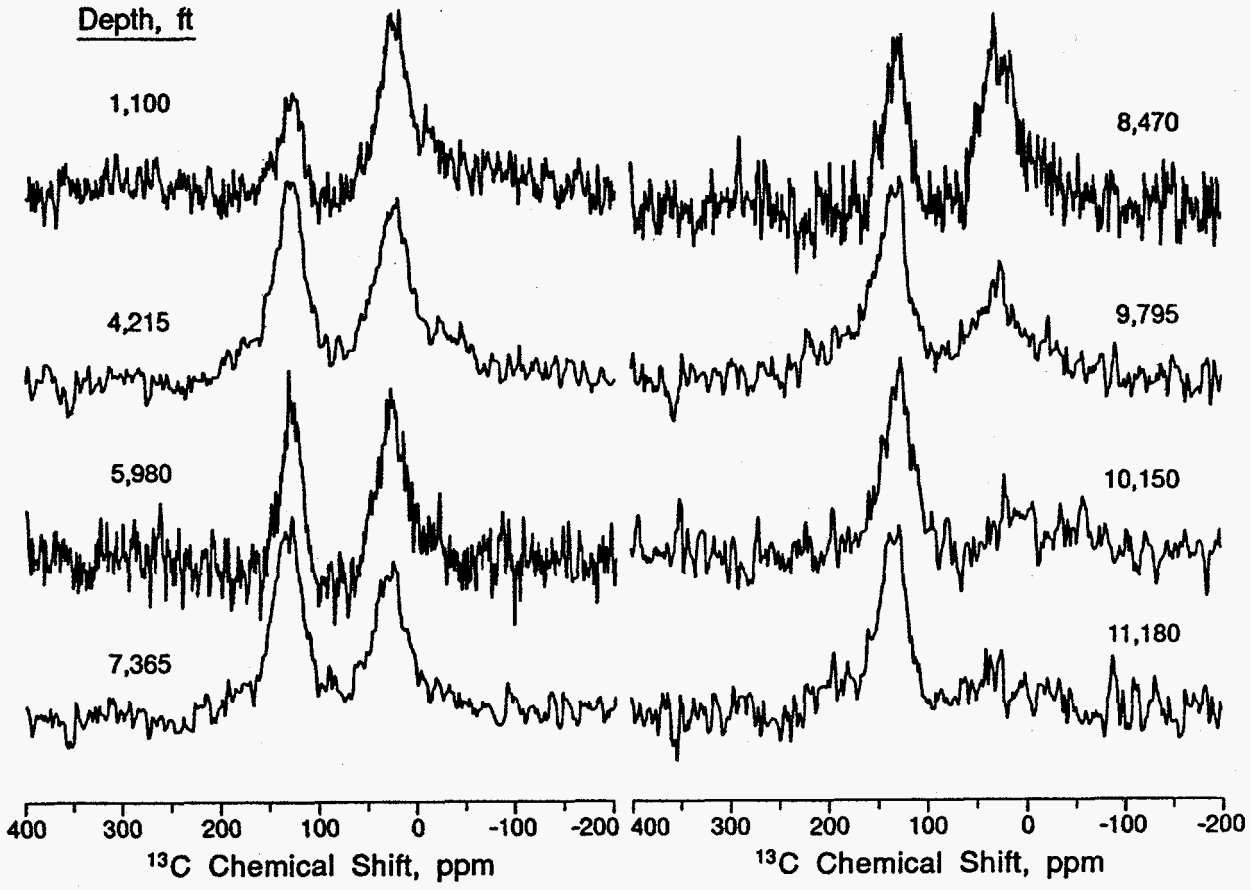

Figure 2. CP/MAS ^{13}C NMR spectra of Bighorn Basin samples from different depths

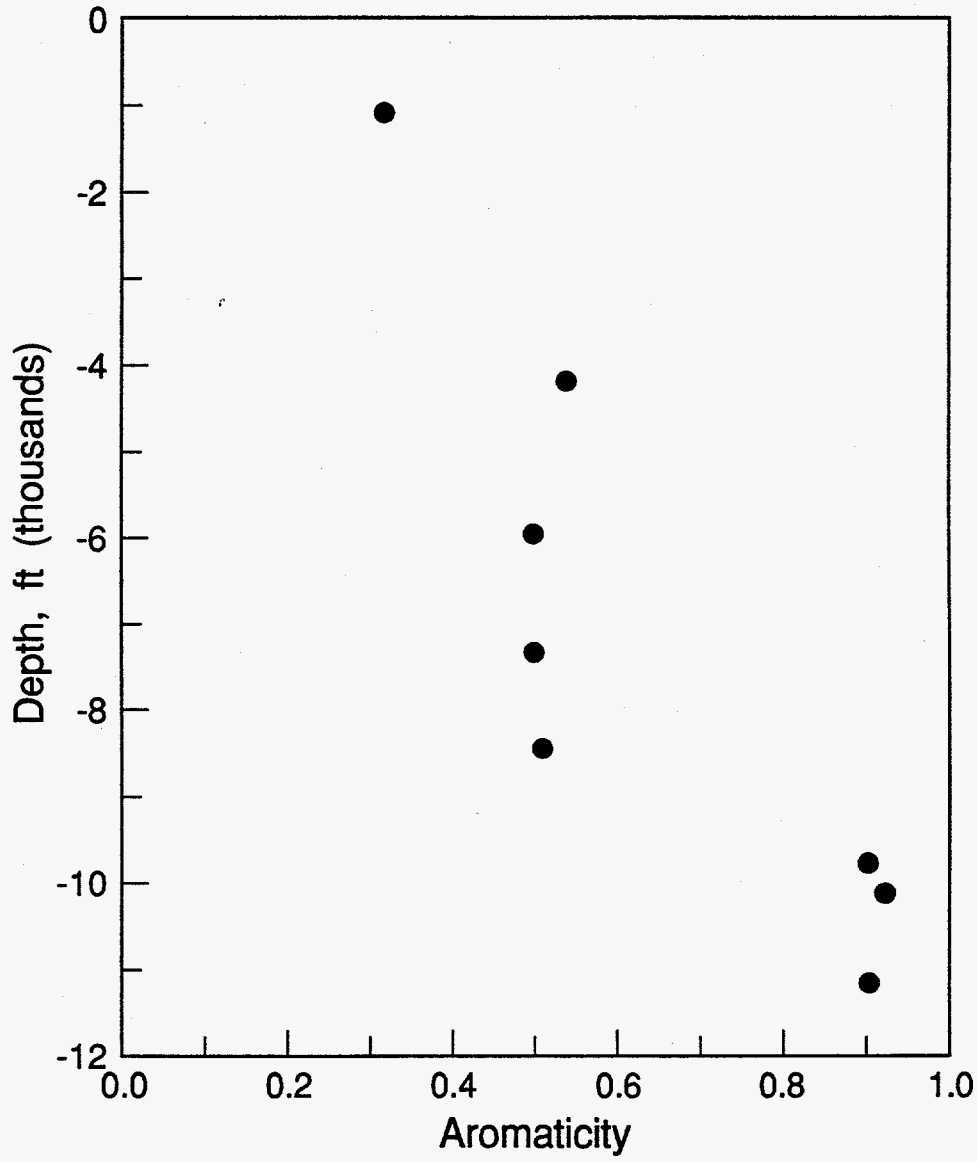

Figure 3. Plot of aromaticity versus depth of burial of Bighorn Basin samples

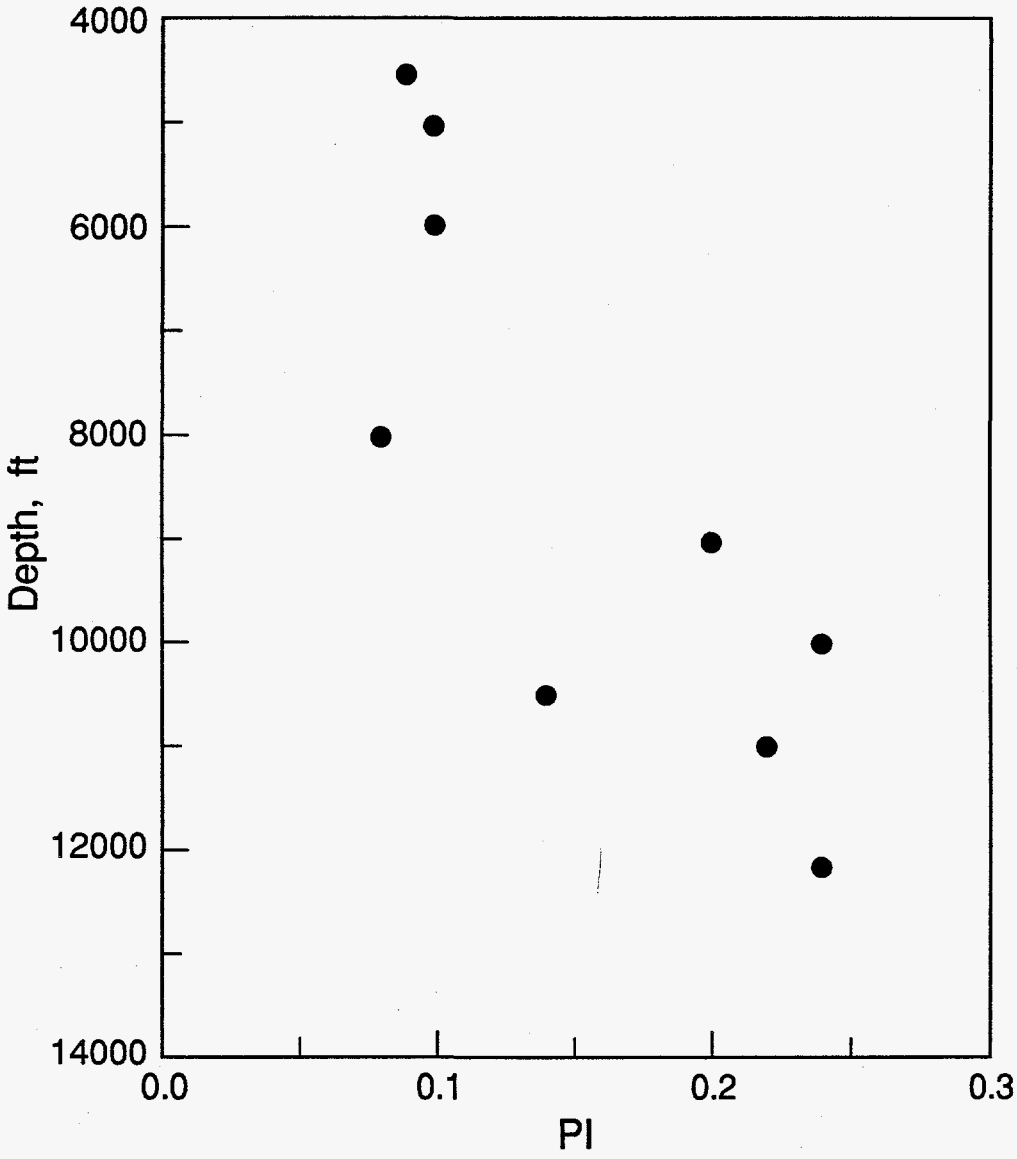

Figure 4. Plot of production index versus depth of burial of Bighorn Basin samples

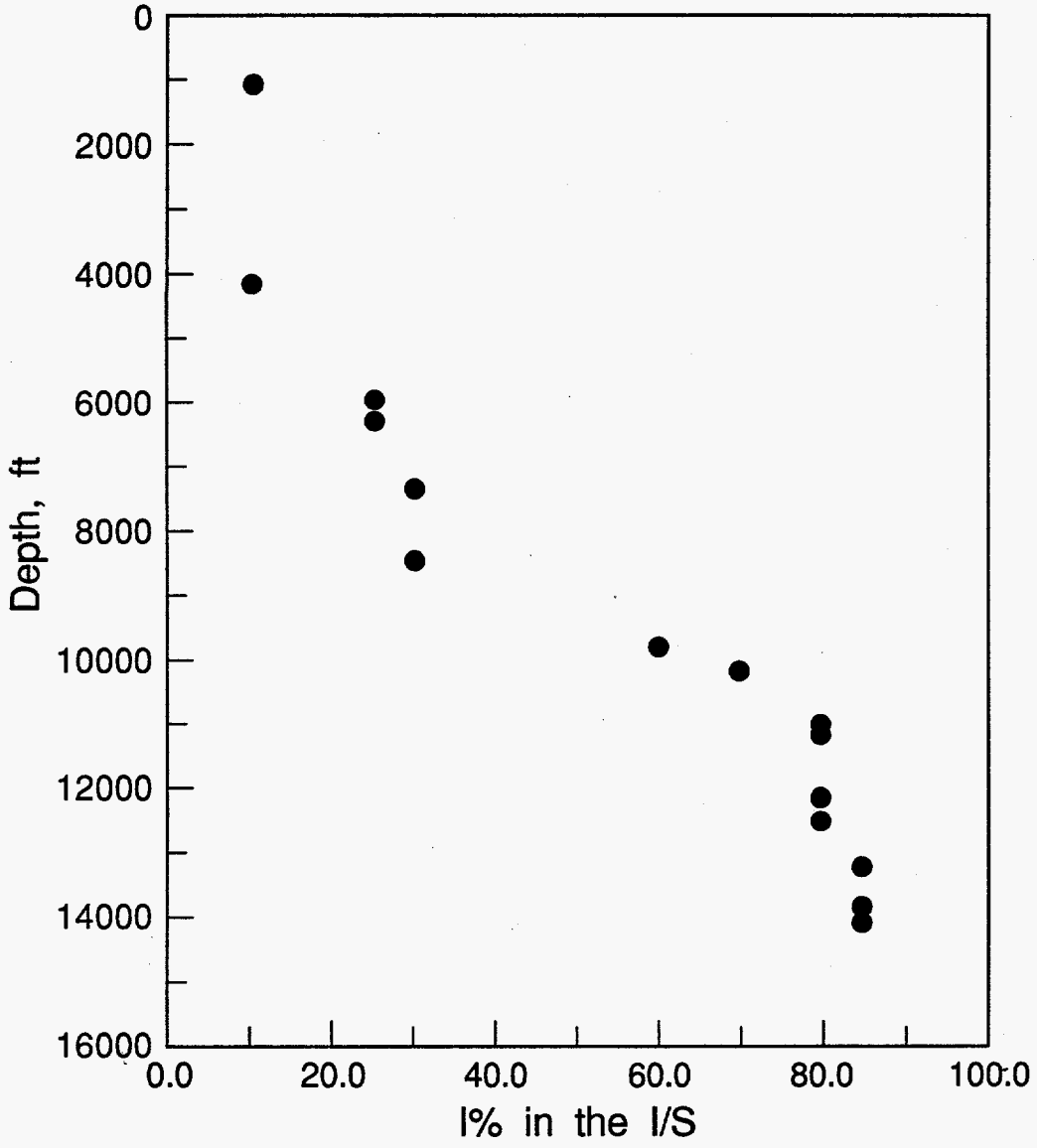

Figure 5. Plot of illite/smectite ratio versus depth of burial of Bighorn Basin samples

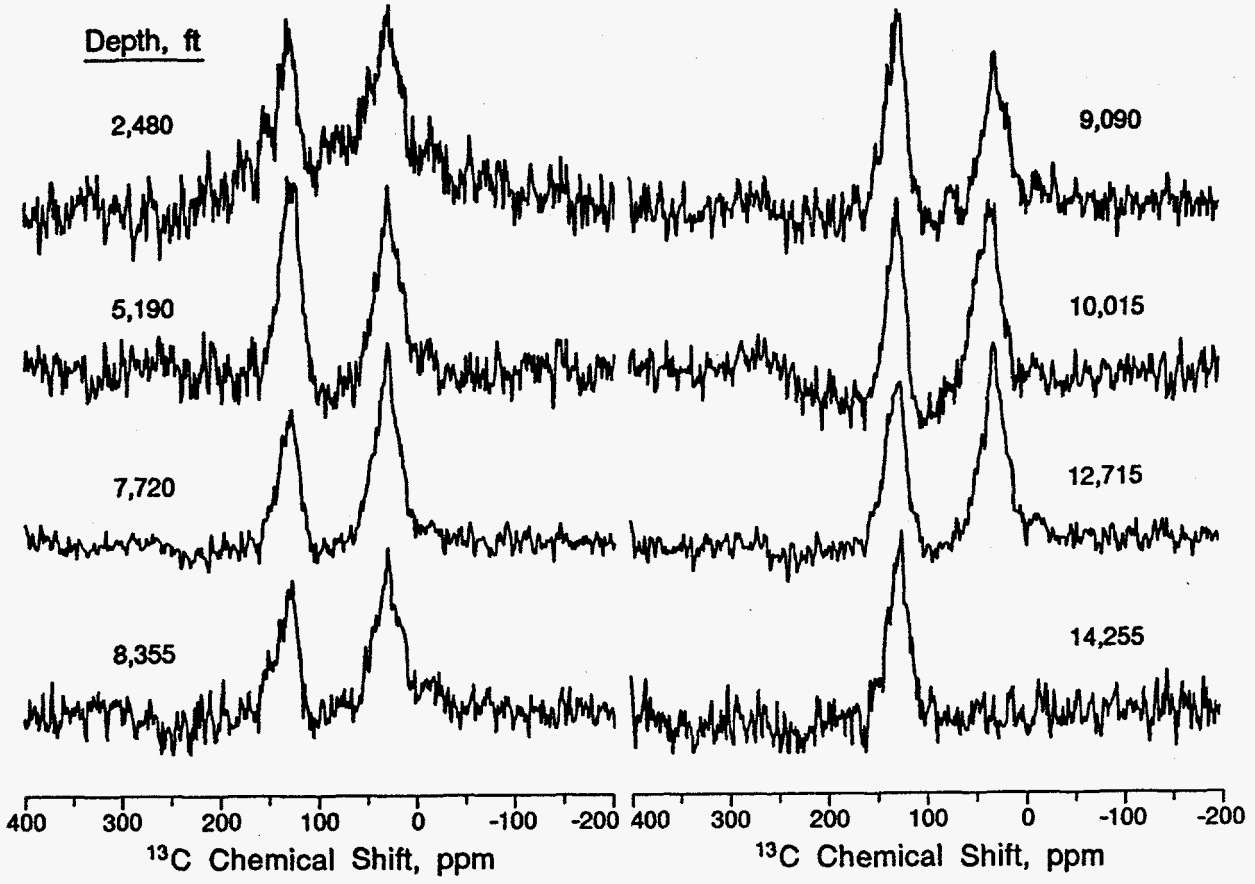

Figure 6. CP/MAS ^{13}C NMR spectra of Wind River Basin samples from different depths

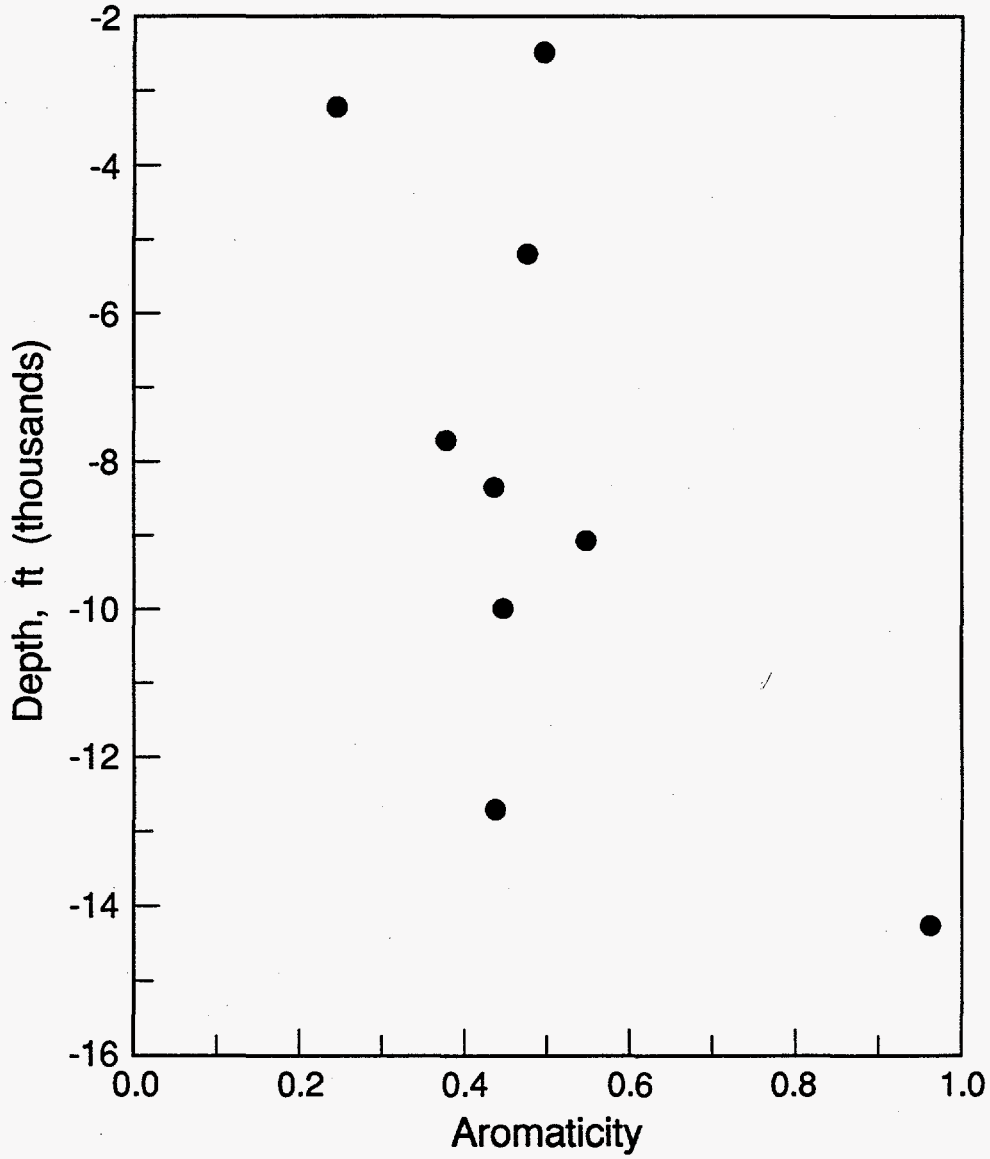

Figure 7. Plot of aromaticity versus depth of burial of Wind River Basin samples

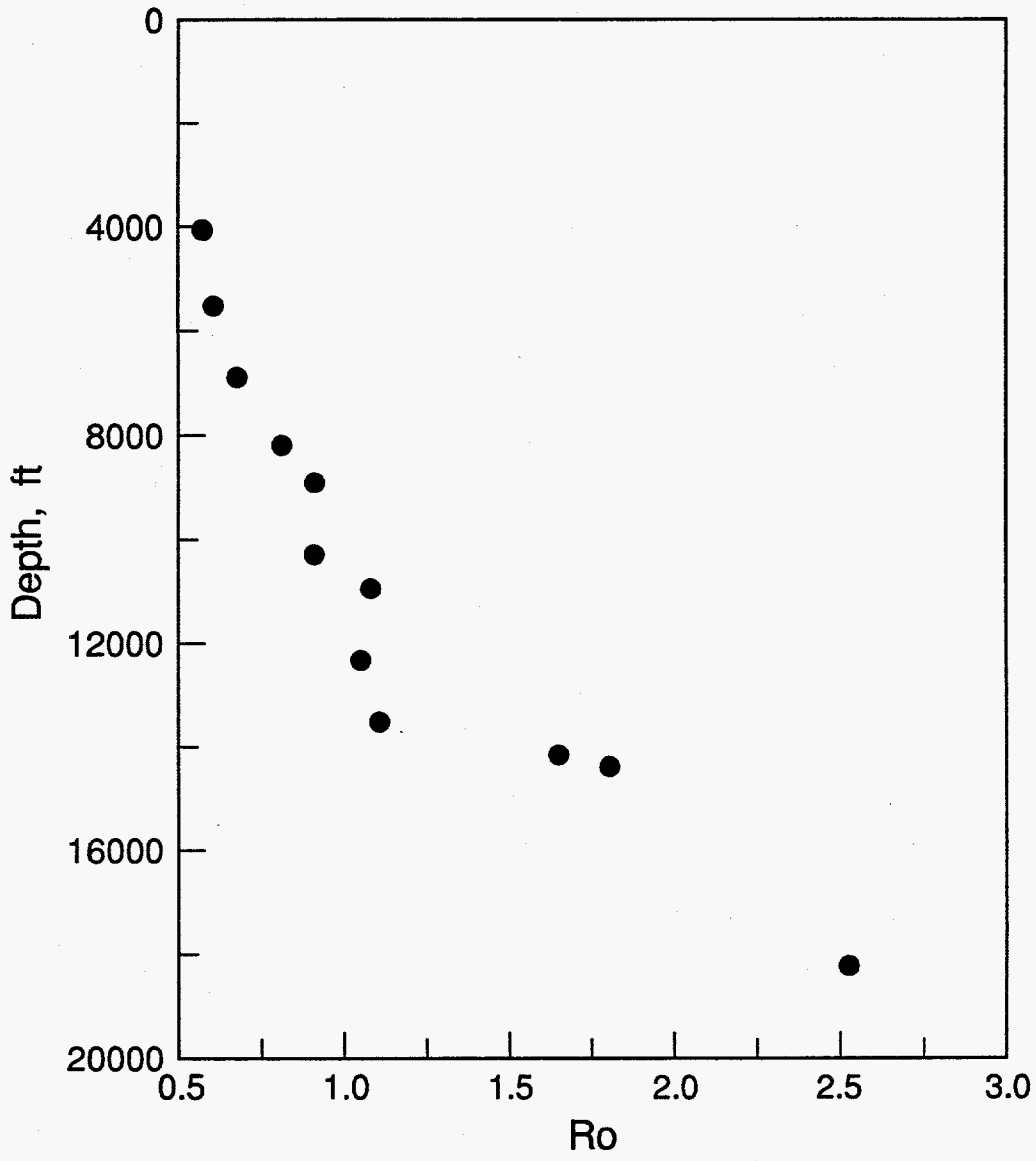

Figure 8. Plot of vitrinite reflectance versus depth of burial of Wind River Basin samples

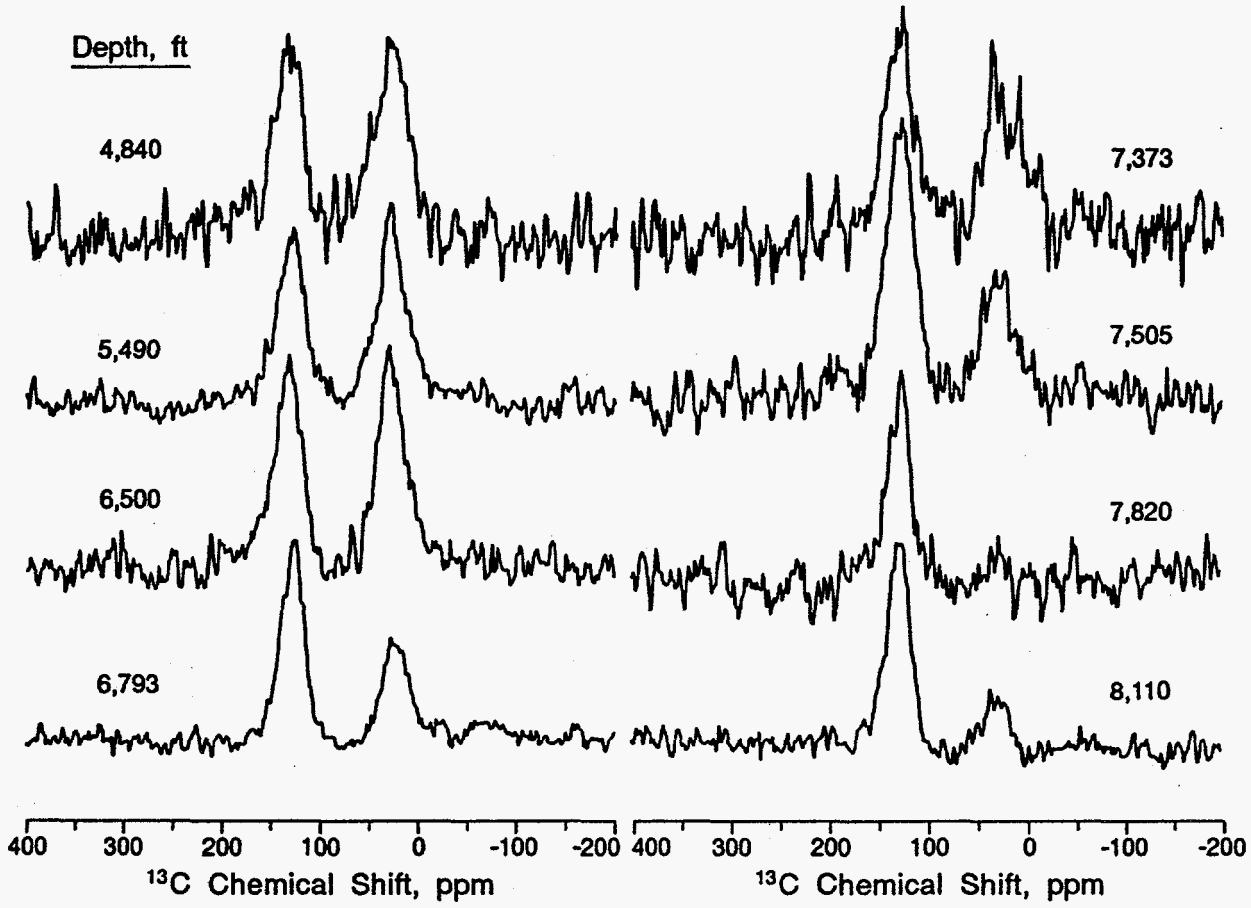

Figure 9. CP/MAS ^{13}C NMR spectra of samples from different depths of the Mowry/ Huntsman Formation, Denver Basin

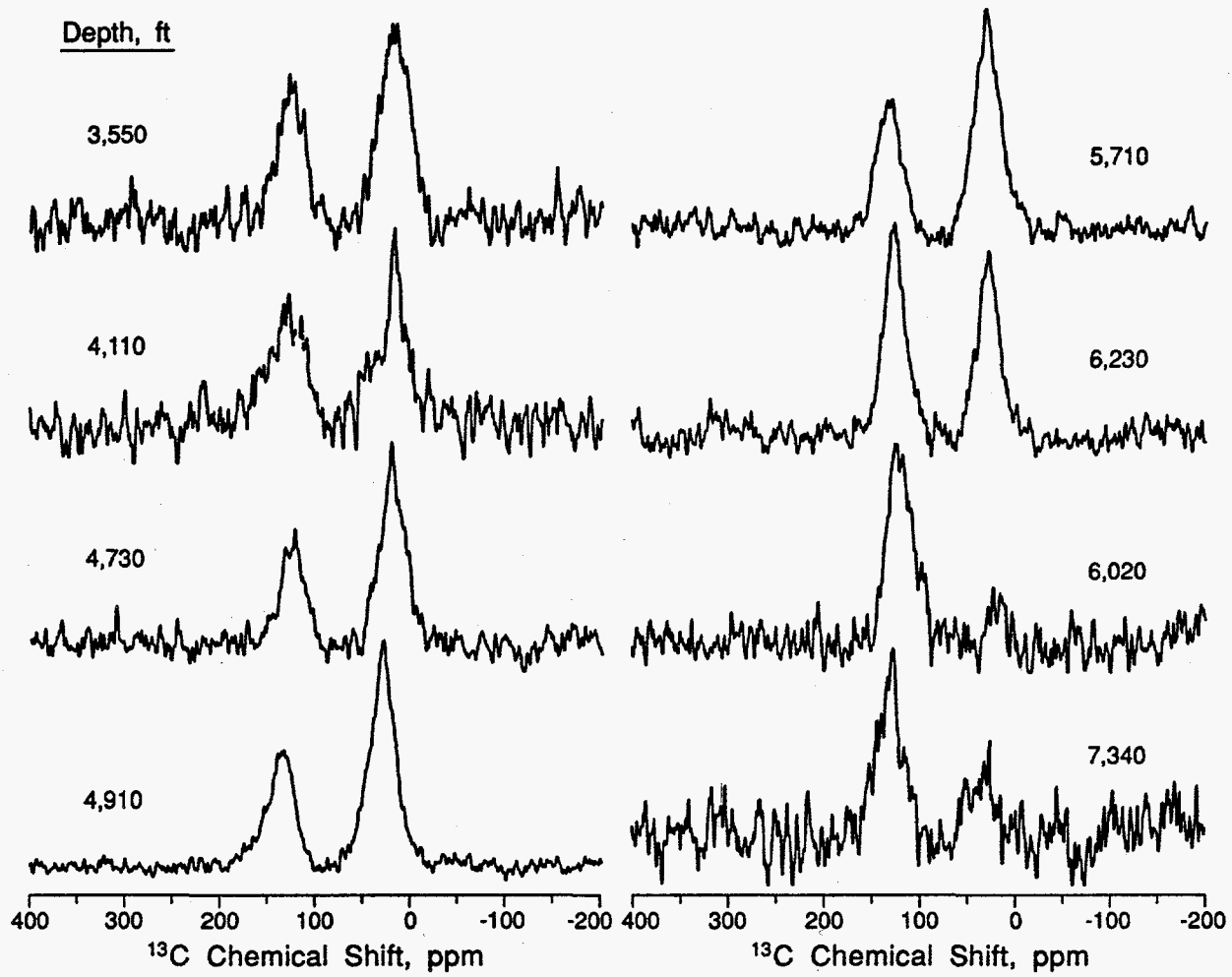

Figure 10. CP/MAS ^{13}C NMR spectra of samples from different depths of the Niobrara Formation, Denver Basin

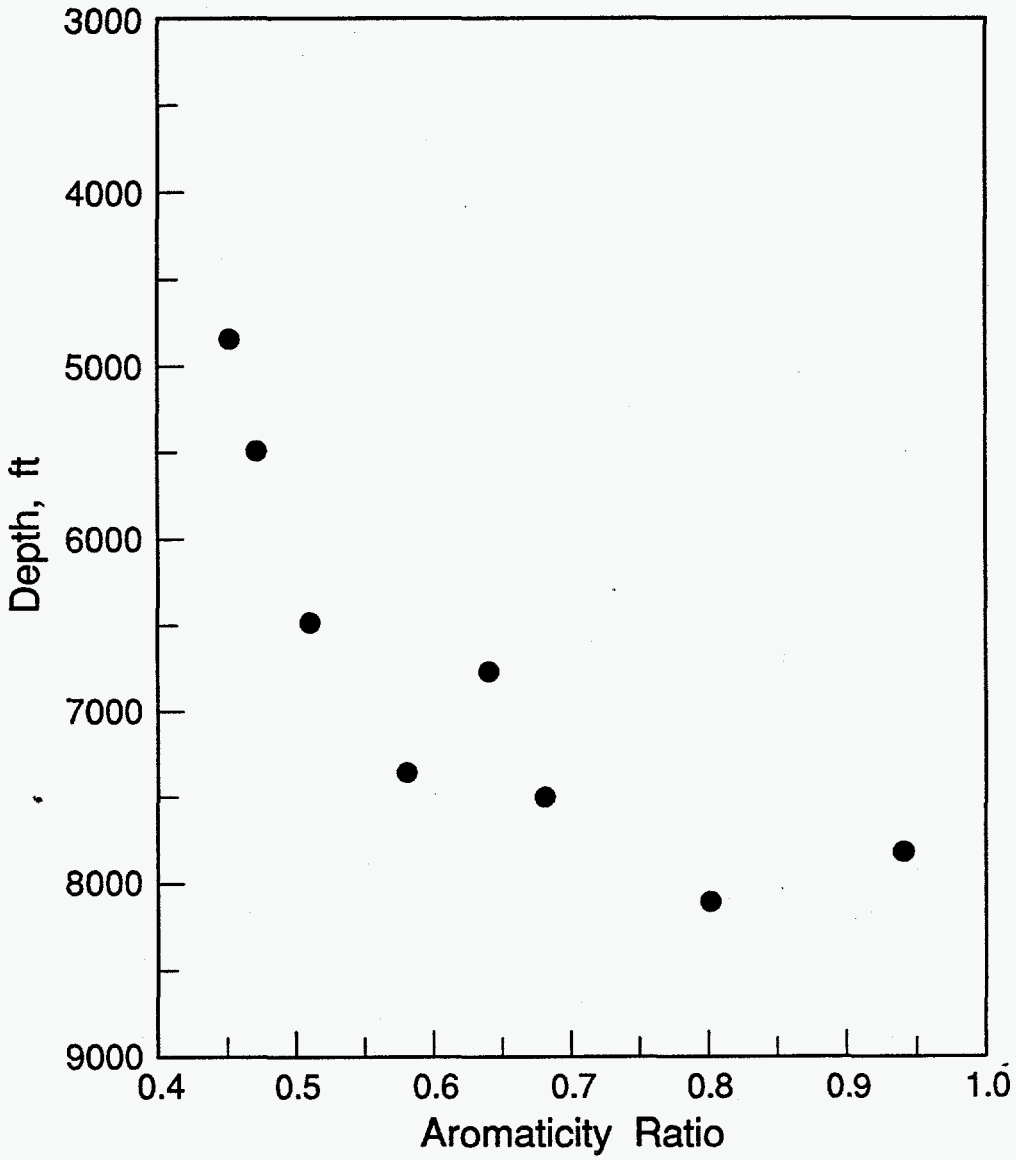

Figure 11. Plot of aromaticity versus depth of burial of Denver Basin samples

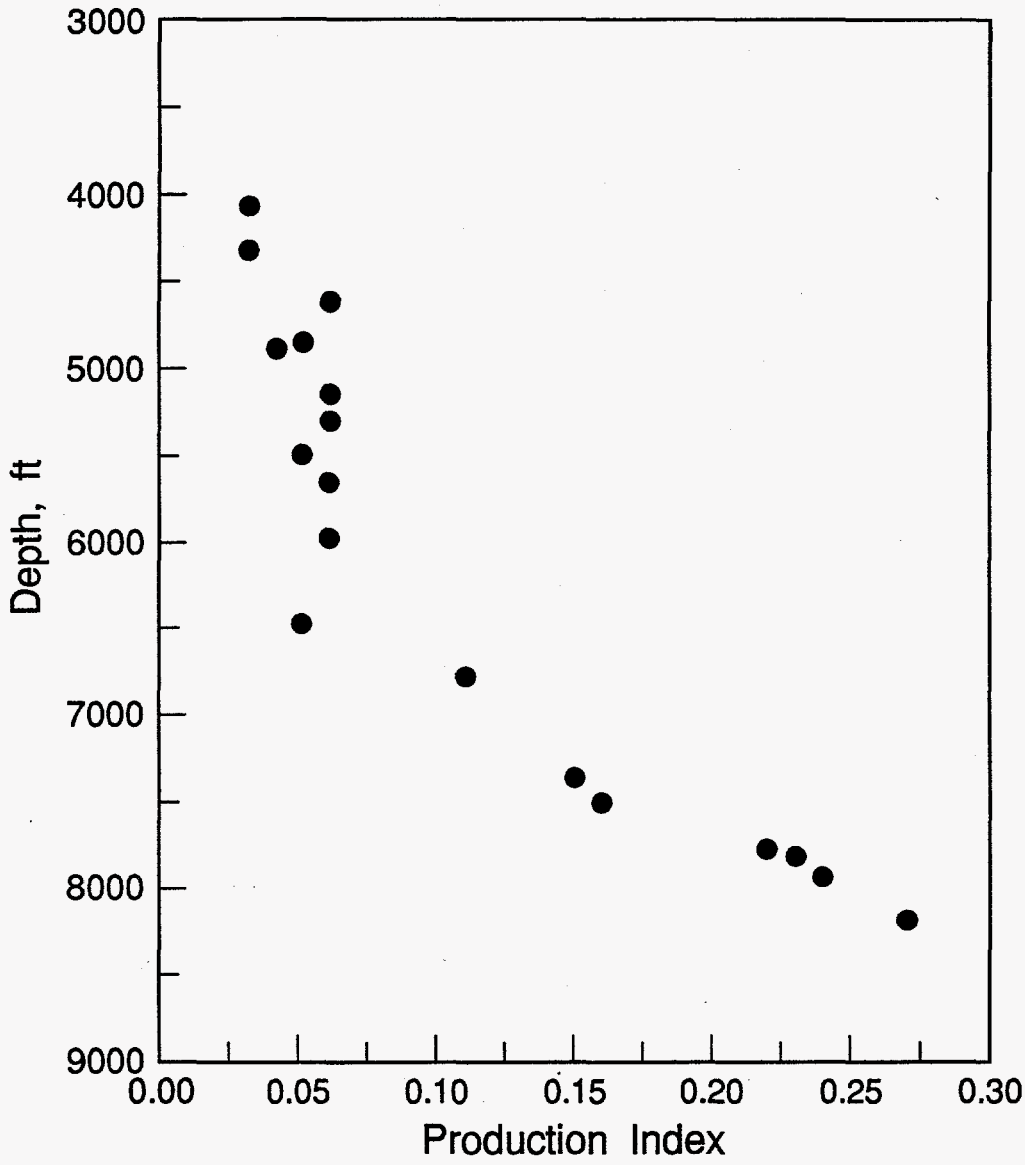

Figure 12. Plot of production index versus depth of burial of Denver Basin samples

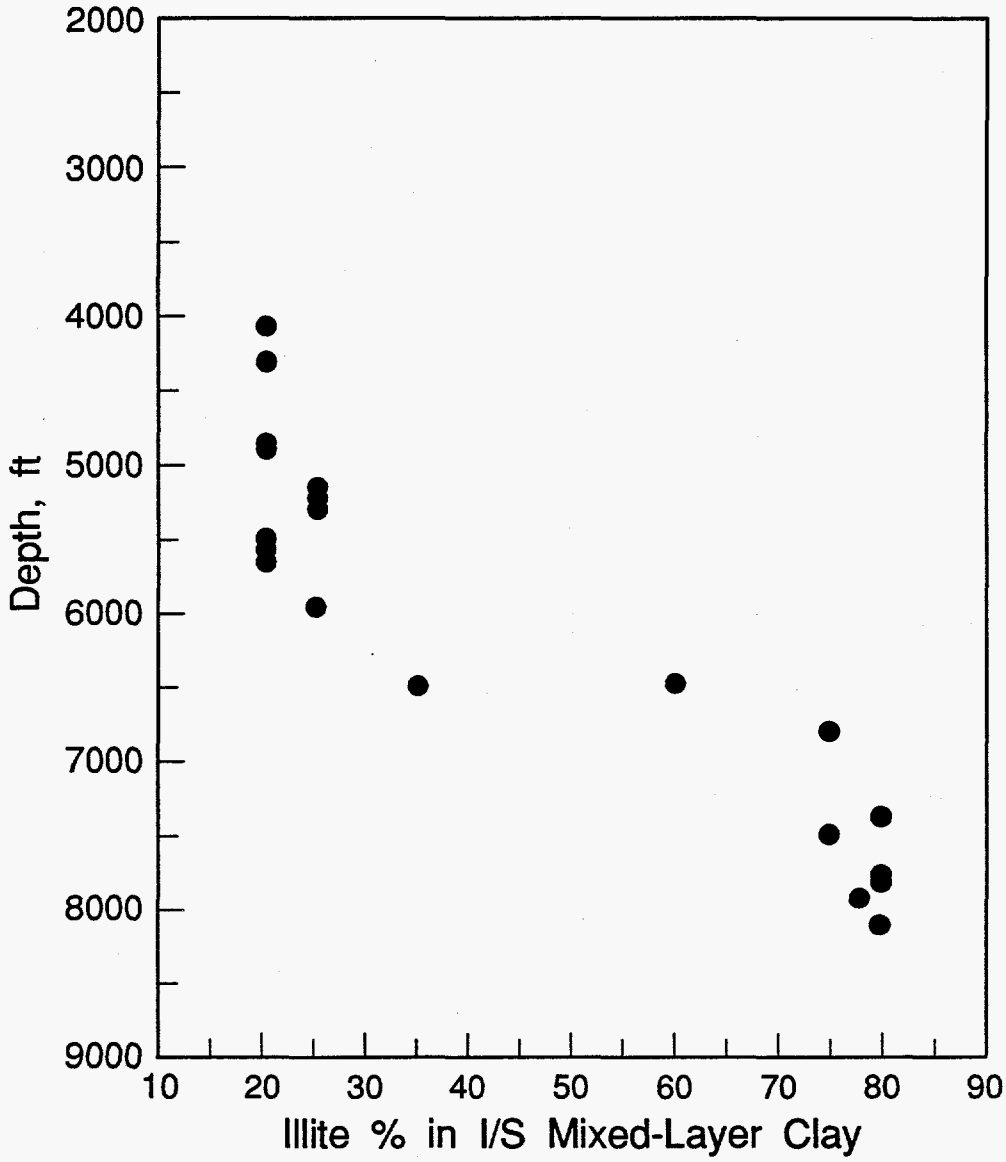

Figure 13. Plot of illite/smectite ratio versus depth of burial of Denver Basin samples

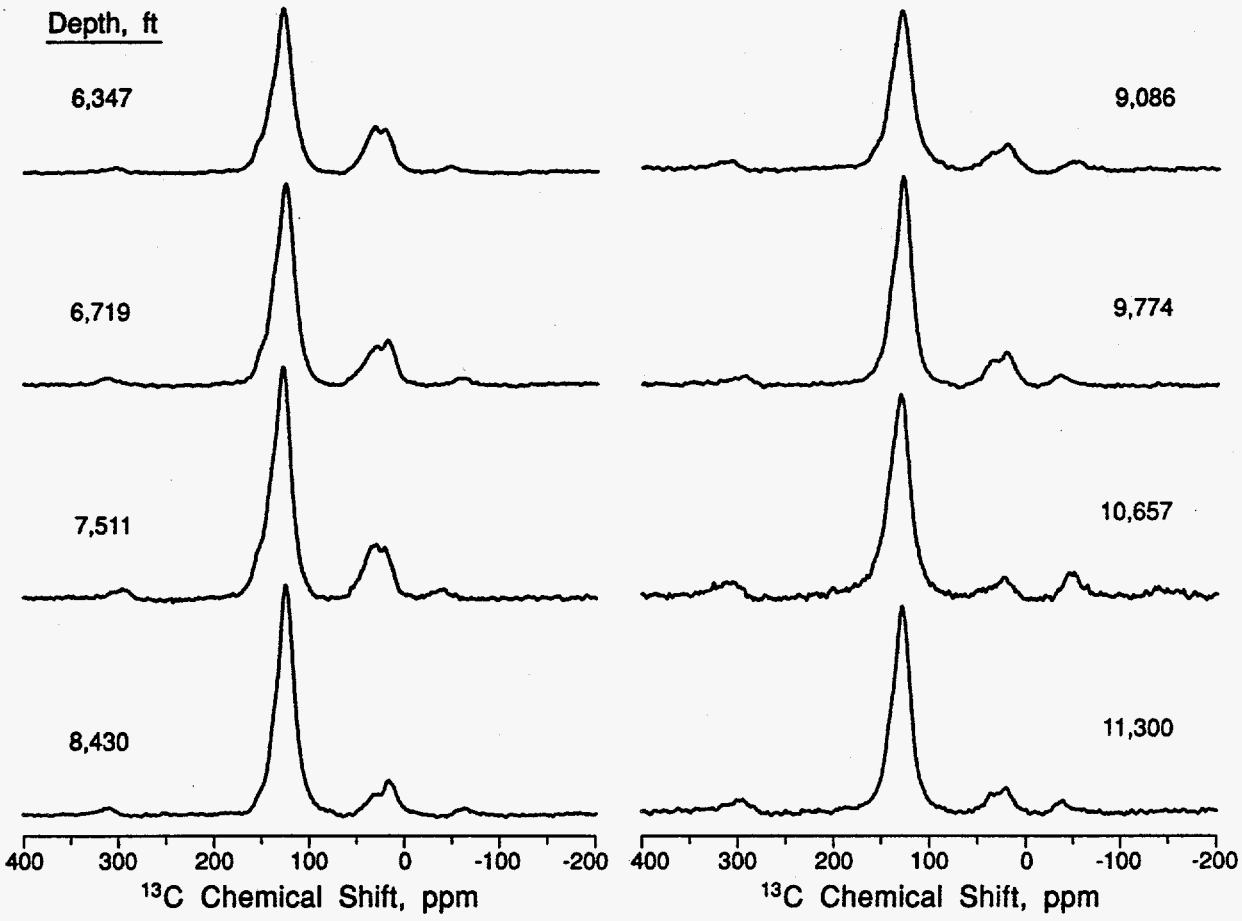

Figure 14. CP/MAS ^{13}C NMR spectra of samples from the Alberta Basin

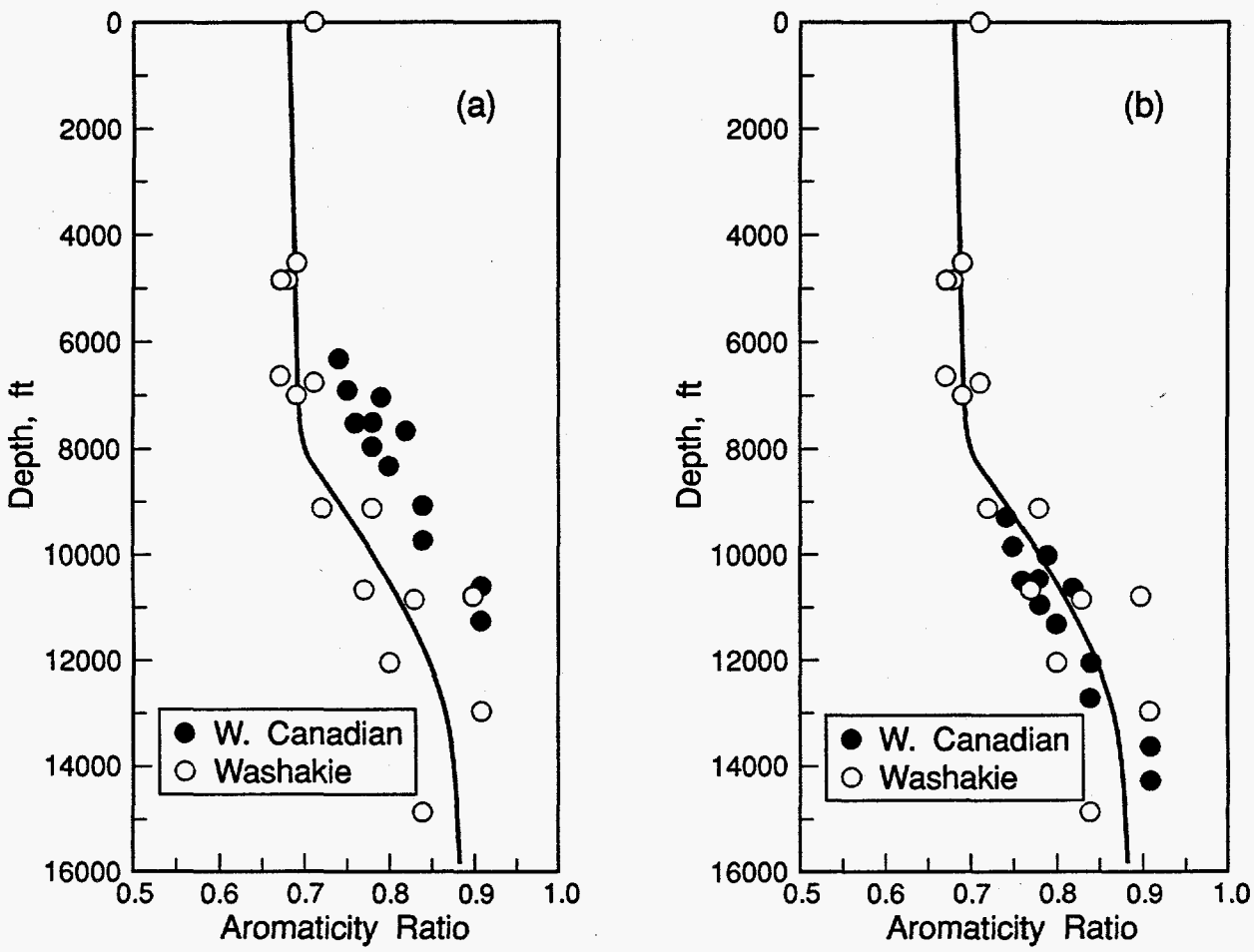

Figure 15. (a) Aromaticity of the Fourth Coal versus depth in the Western Canada Basin. Data from the Washakie Basin are plotted for reference. (b) Application of a 3000-ft (915-m) uplift to the Western Canada Basin coals. (From Jiao et al. 1996)

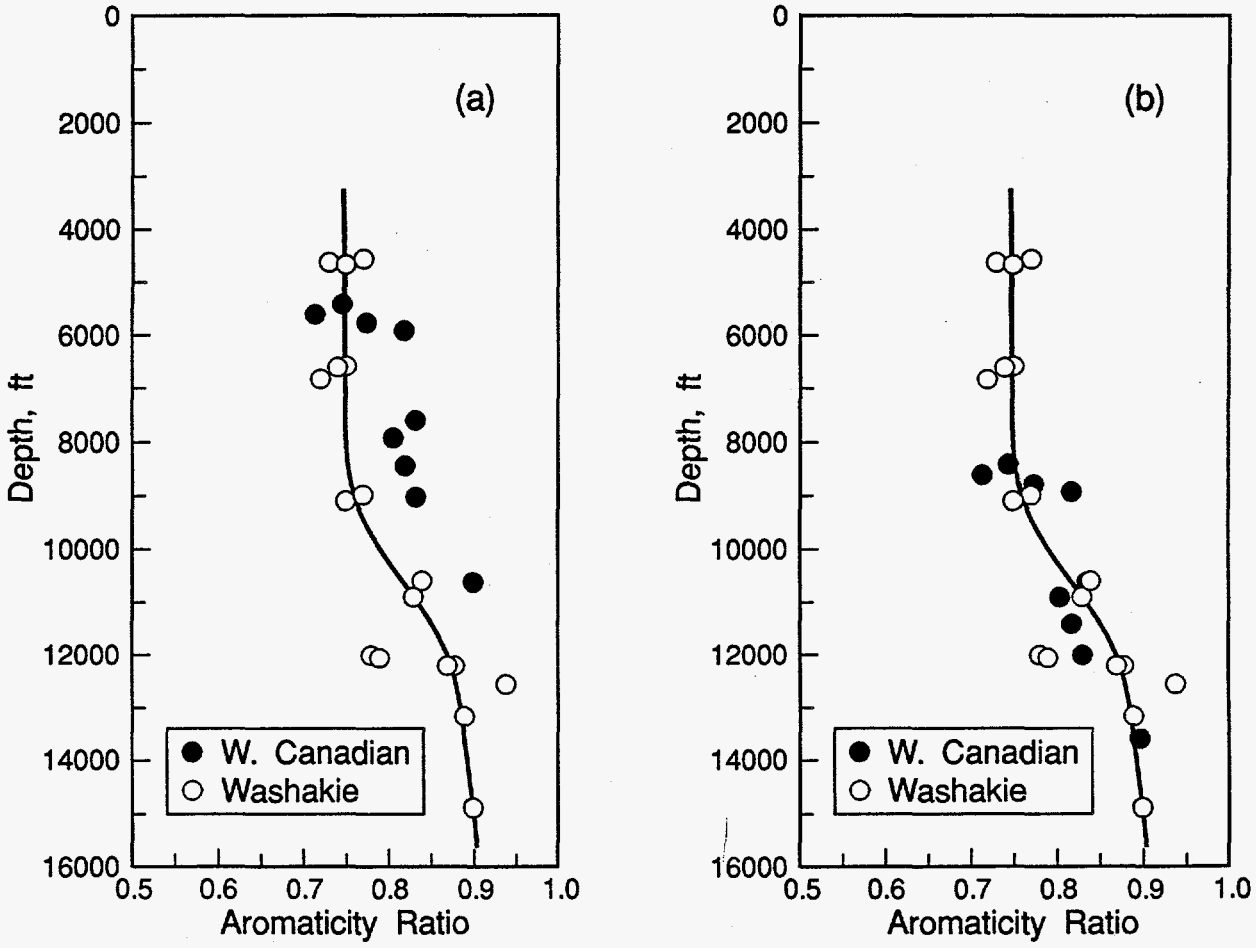

Figure 16. (a) Aromaticity of the Fish Scale zone versus depth in the Western Canada Basin. Data from the Washakie Basin are plotted for reference. (b) Application of a 3000-ft (915-m) uplift to the Western Canada Basin coals. (From Jiao et al. 1996)

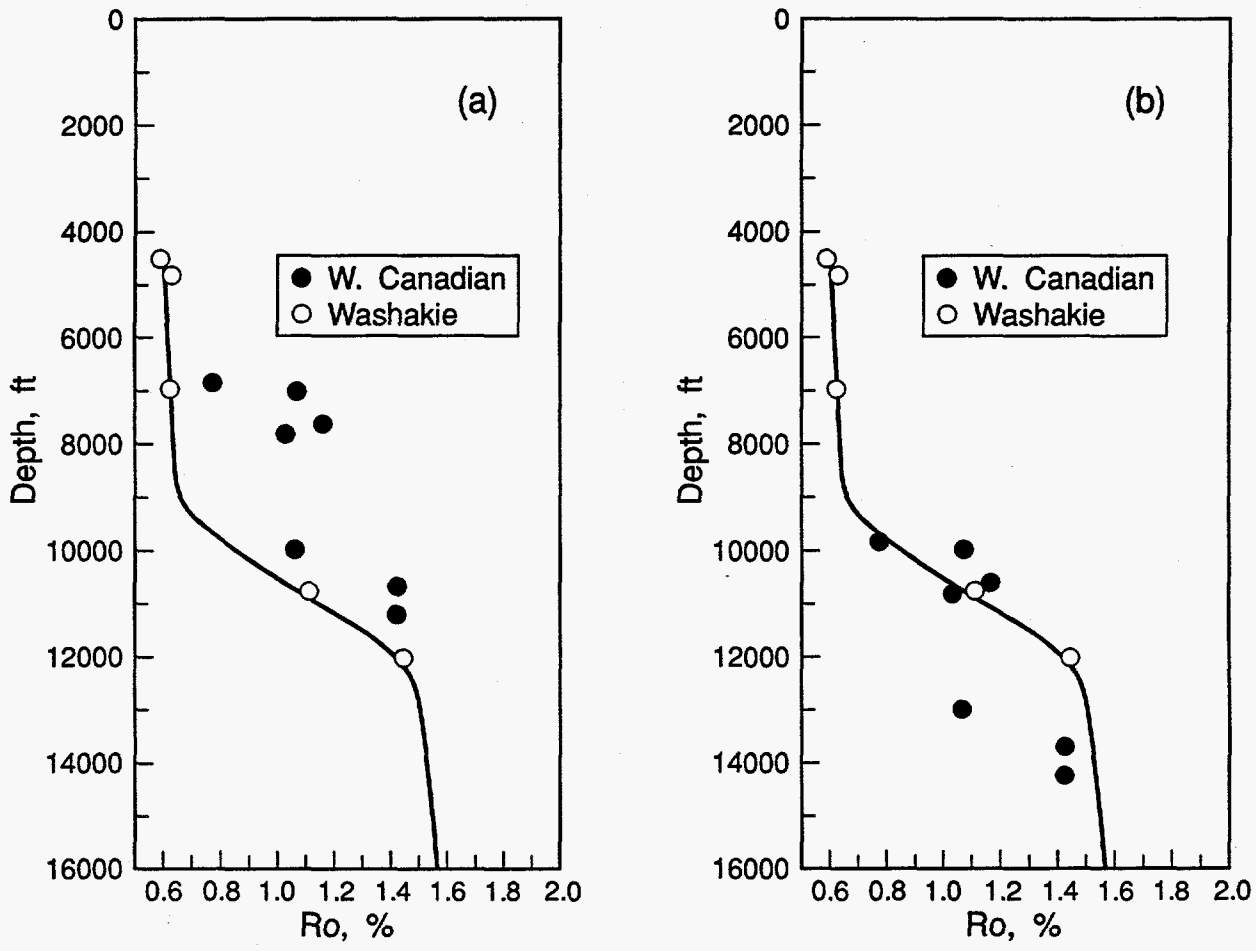

Figure 17. (a) Vitrinite reflectance of the Fourth Coal versus depth in the Western Canada Basin. Data from the Washakie Basin are plotted for reference. (b) Application of a 3000-ft (915-m) uplift to the Western Canada Basin coals. (From Jiao et al. 1996)

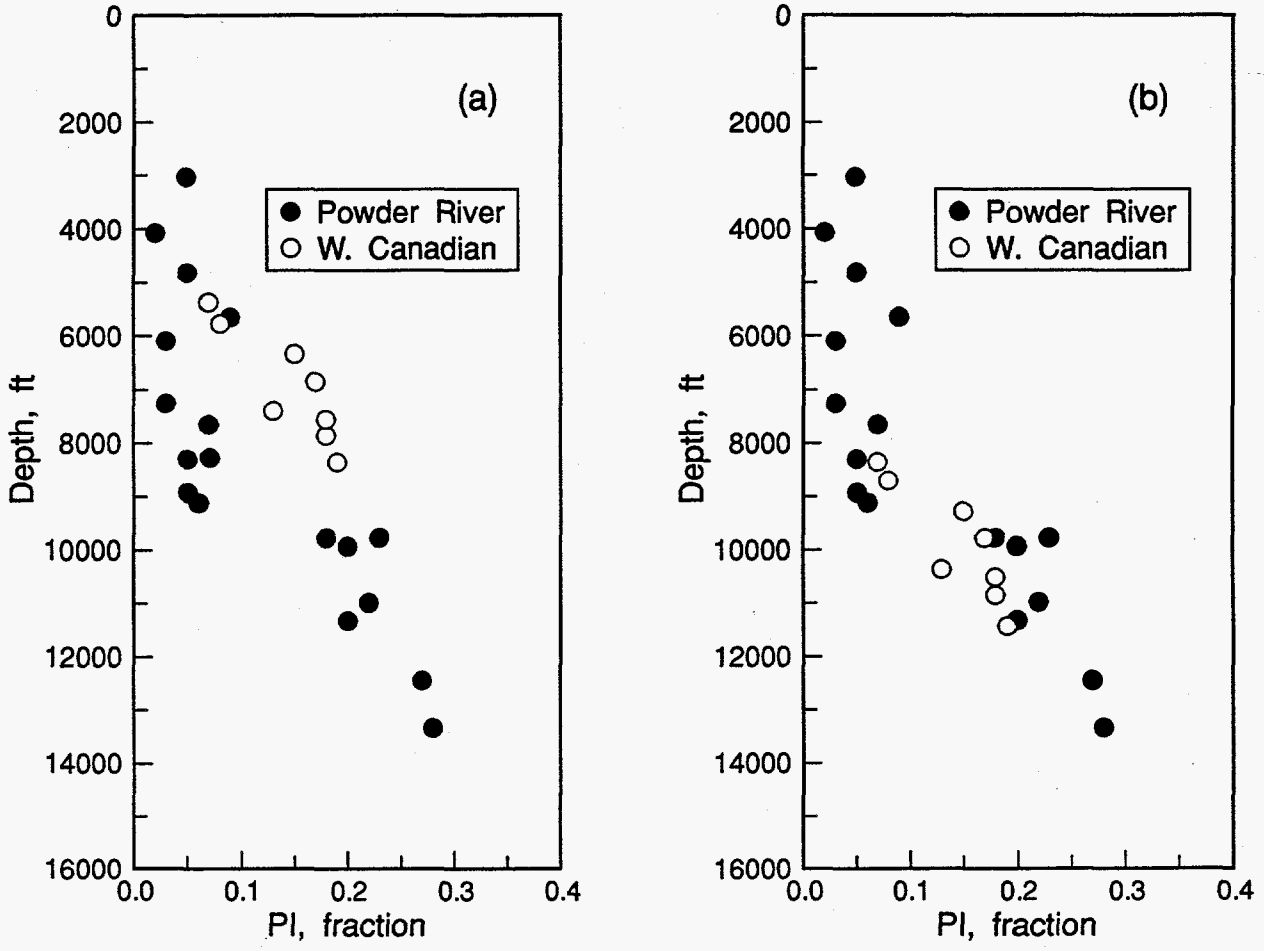

Figure 18. (a) Production index of the Cretaceous shales versus depth in the Western Canada Basin. Data from the Washakie Basin are plotted for reference. (b) Application of a 3000-ft (915-m) uplift to the Western Canada Basin coals. (From Jiao et al. 1996)

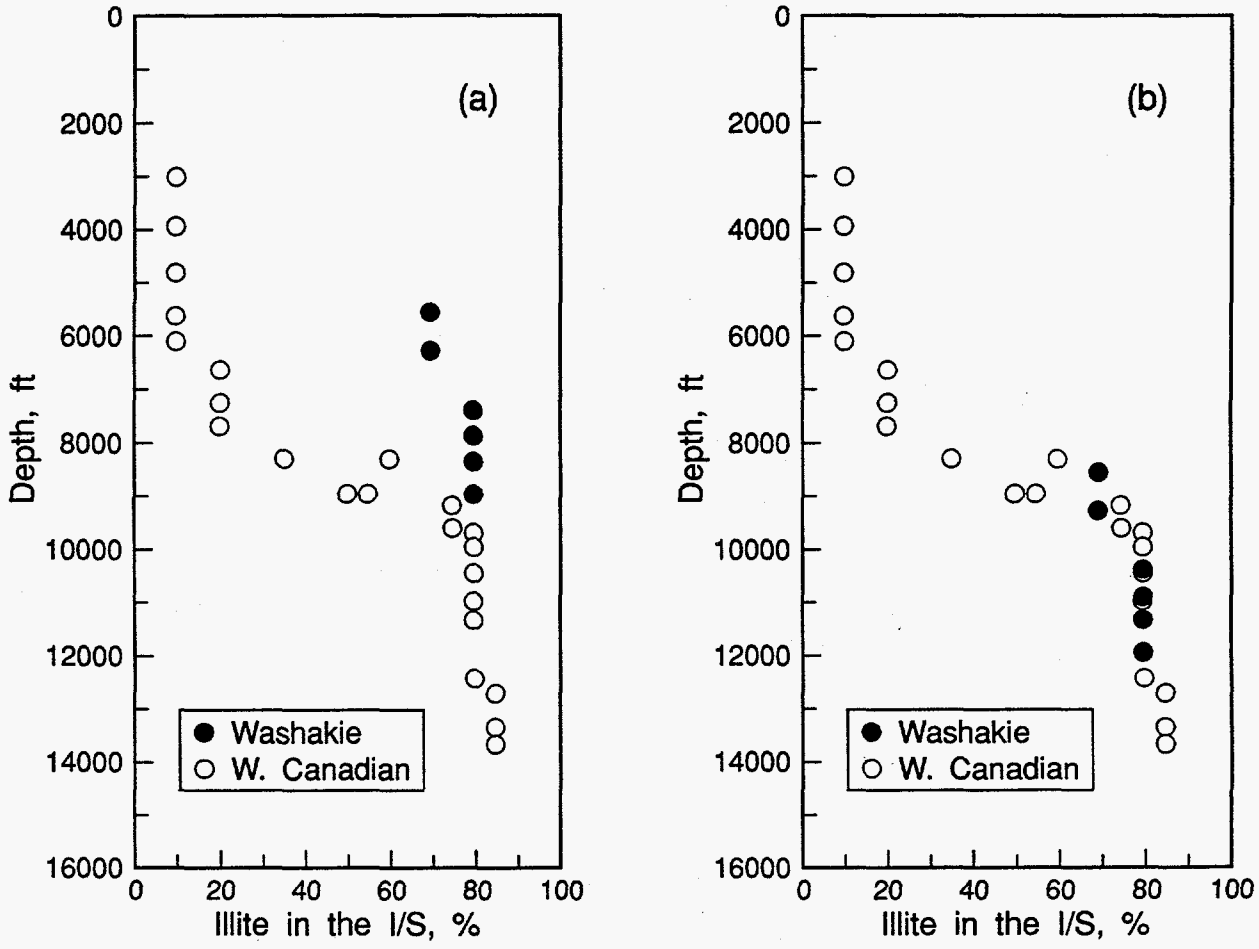

Figure 19. **(a) Percent illite in the smectite/illite mixed-layer clays versus depth in the Western Canada Basin. Data from the Washakie Basin are plotted for reference. (b) Application of a 3000-ft (915-m) uplift to the Western Canada Basin coals. (From Jiao et al. 1996)**

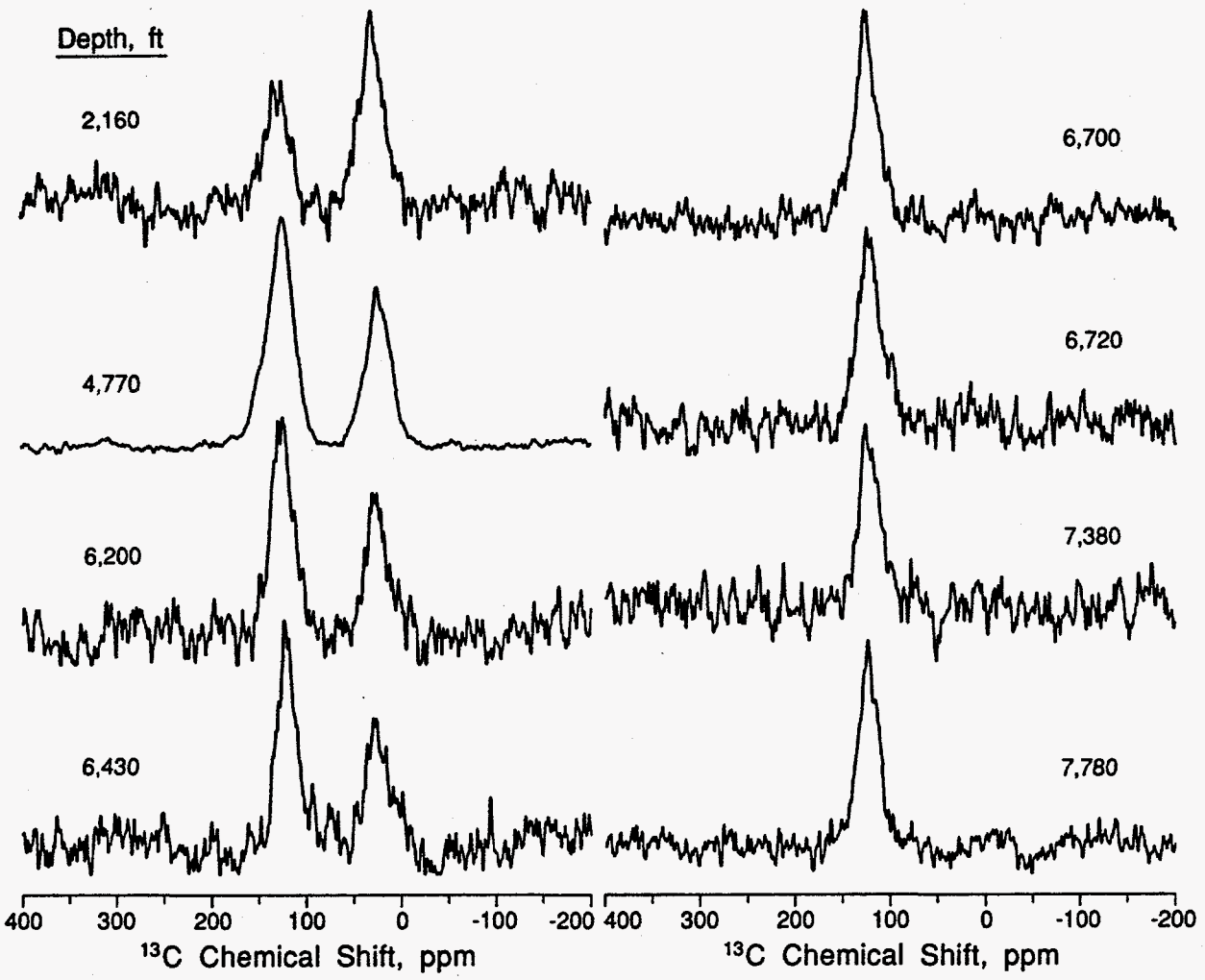

Figure 20. **CP/MAS ^{13}C NMR spectra of San Juan Basin samples from different depths. (Graneros shale)**

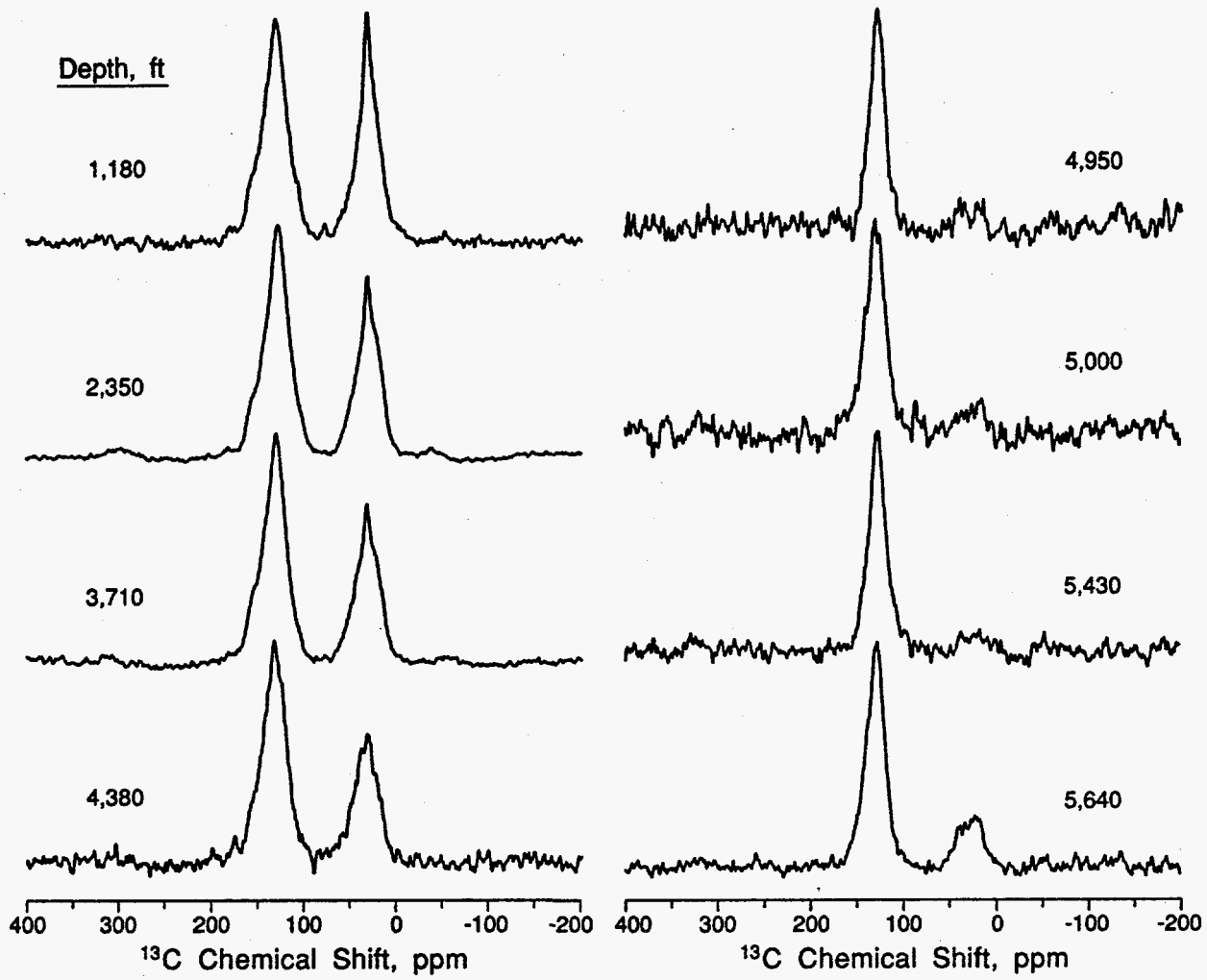

Figure 21. **CP/MAS ^{13}C NMR spectra of San Juan Basin samples from different depths. (Menefee shale)**

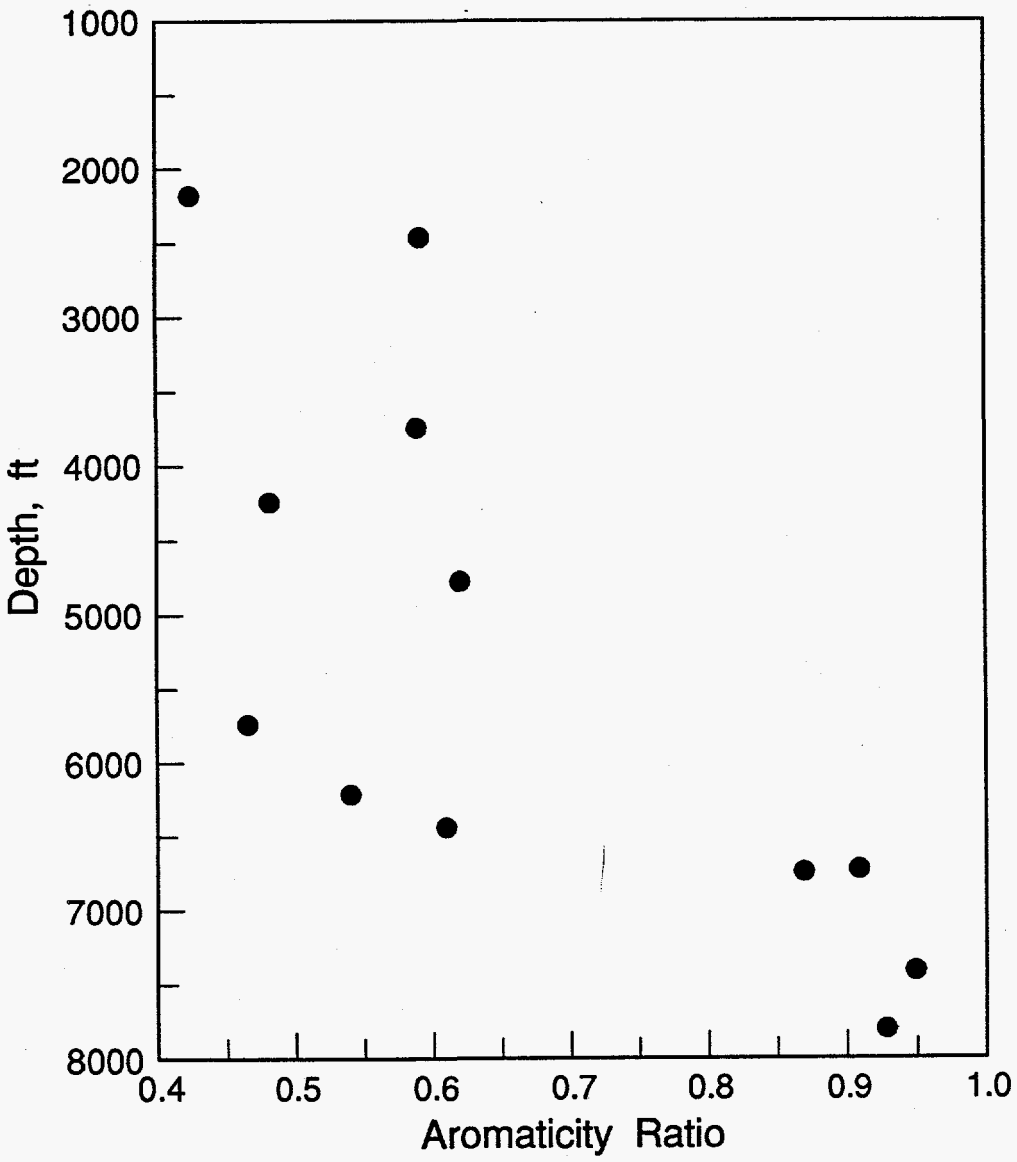

Figure 22. Plot of aromaticity versus depth of burial of San Juan Basin samples. (Graneros shale)

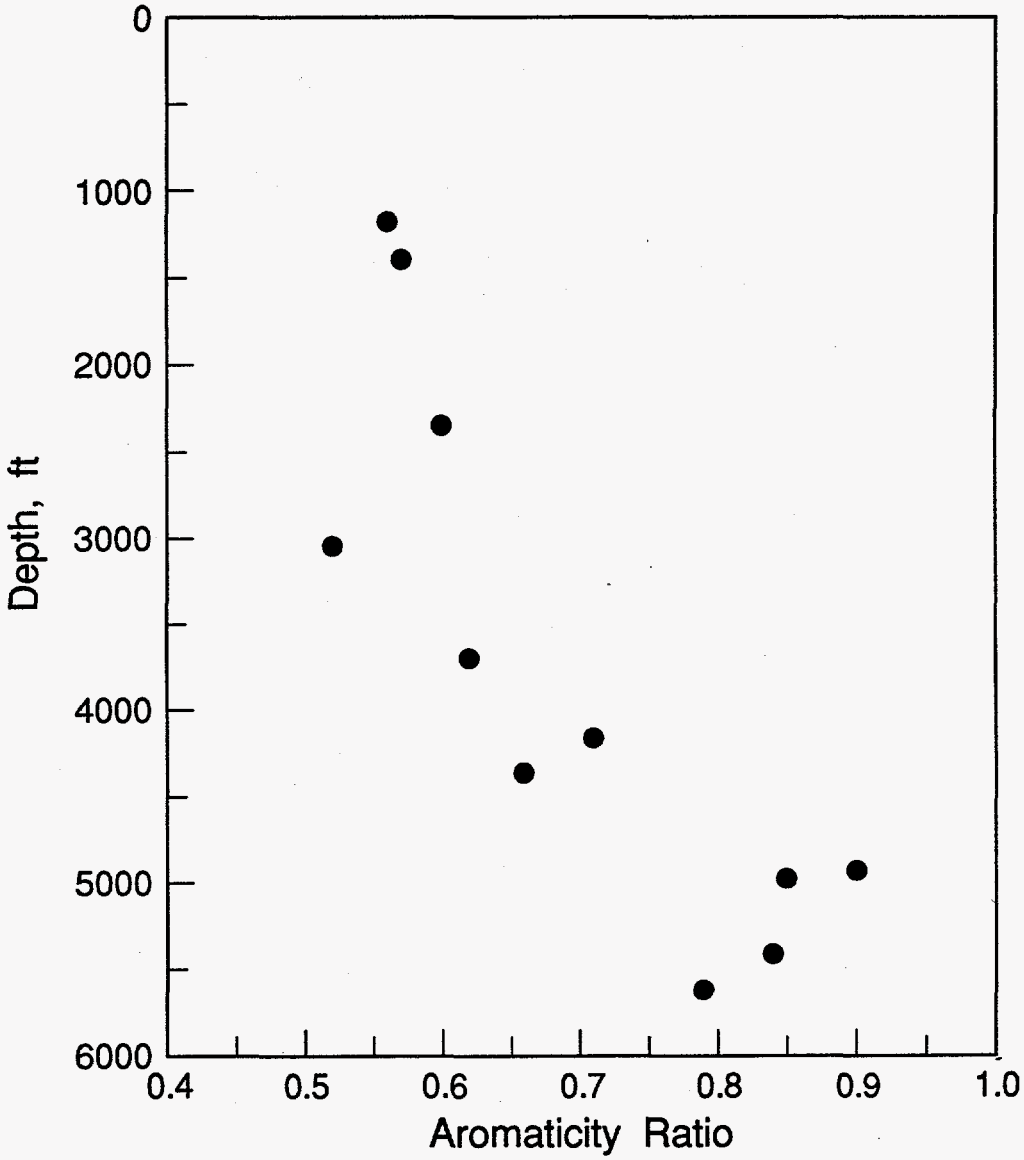

Figure 23. **Plot of aromaticity versus depth of burial of San Juan Basin samples. (Menefee shale)**

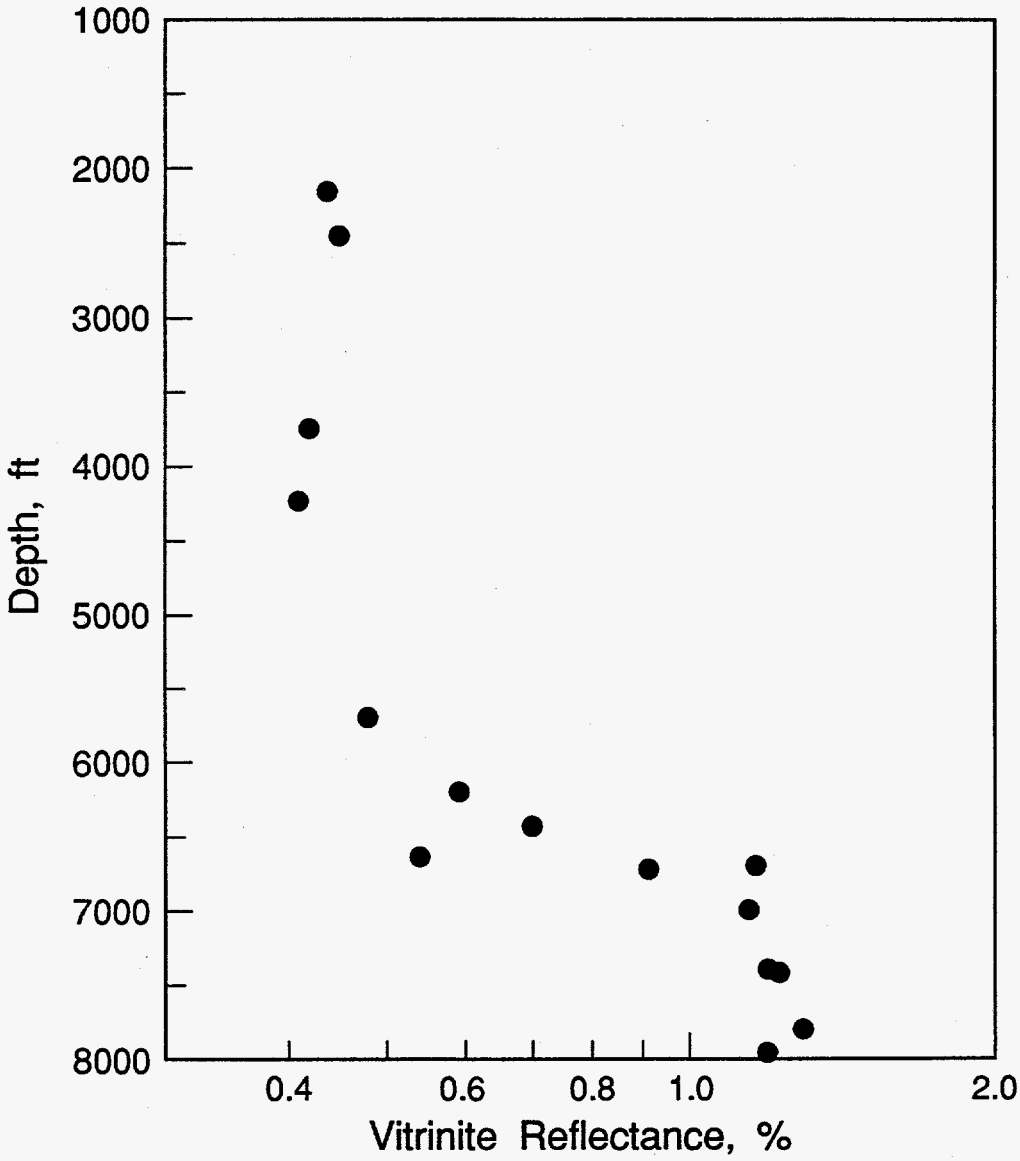

Figure 24. Plot of vitrinite reflectance versus depth of burial of San Juan Basin samples. (Graneros shale)

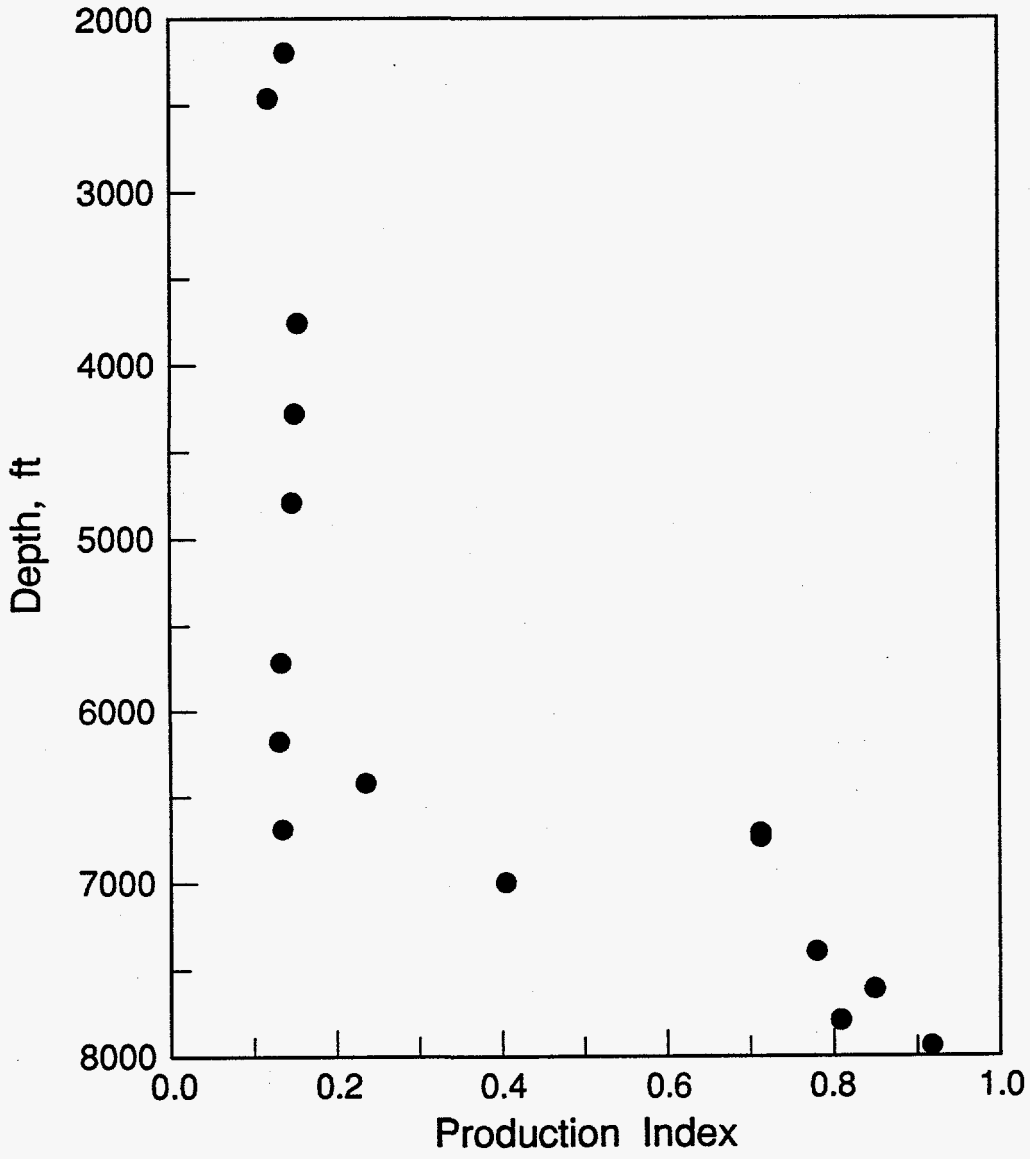

Figure 25. Plot of production index versus depth of burial of San Juan Basin samples. (Graneros shale)

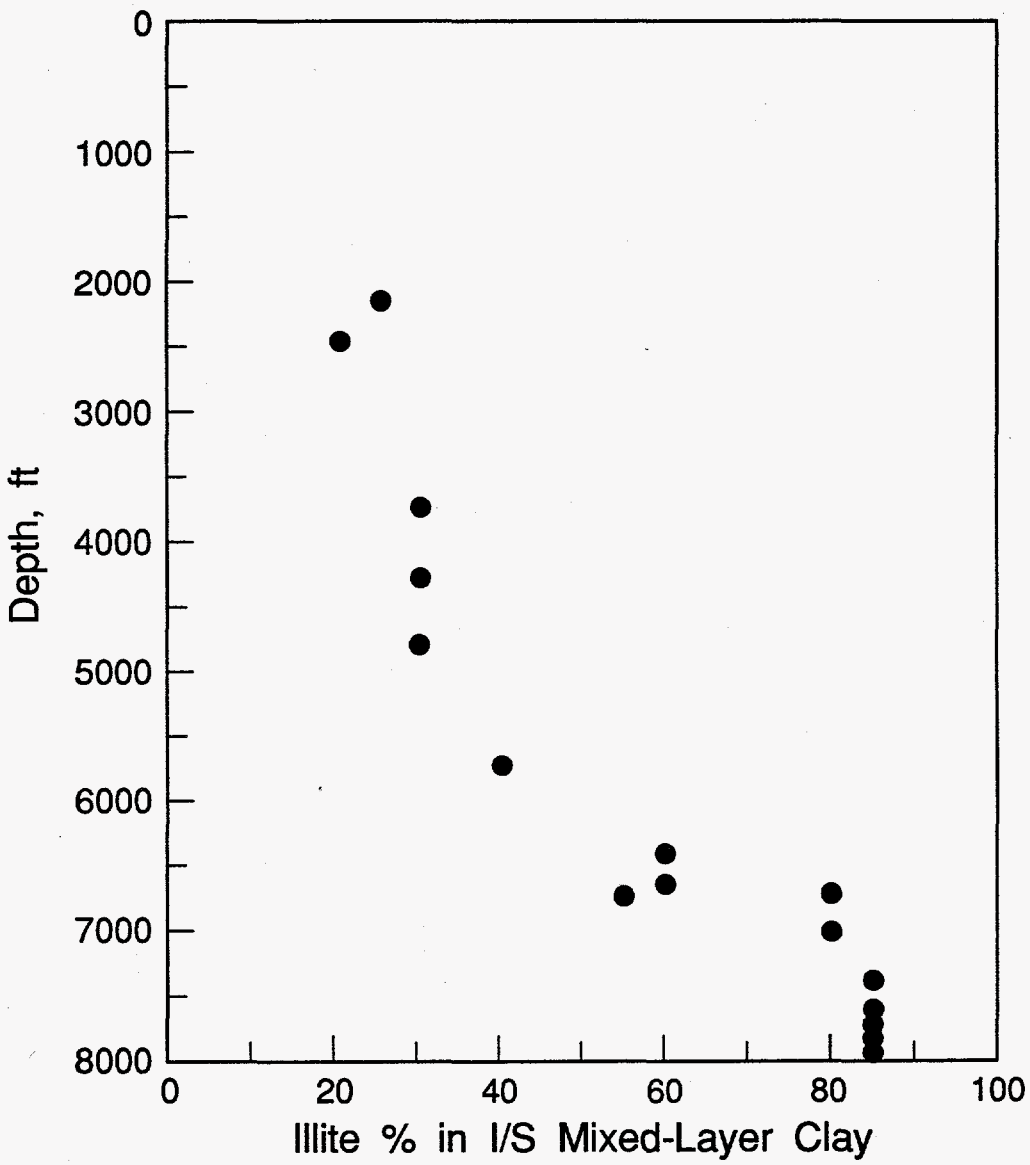

Figure 26. Plot of illite/smectite ratio versus depth of burial of San Juan Basin samples. (Graneros shale)

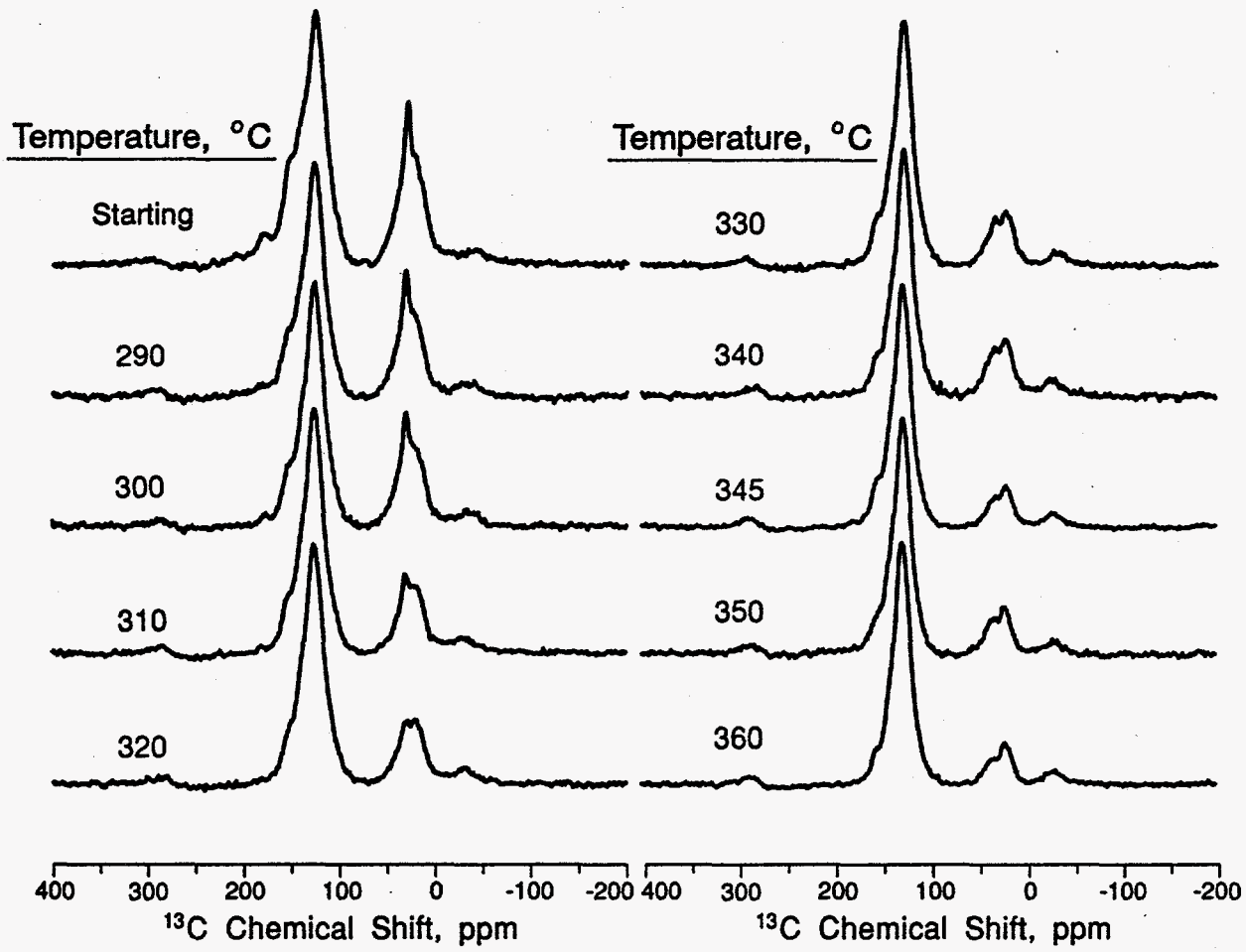

Figure 27. CP/MAS ^{13}C NMR spectra of Almond coal hydrous pyrolysis residues

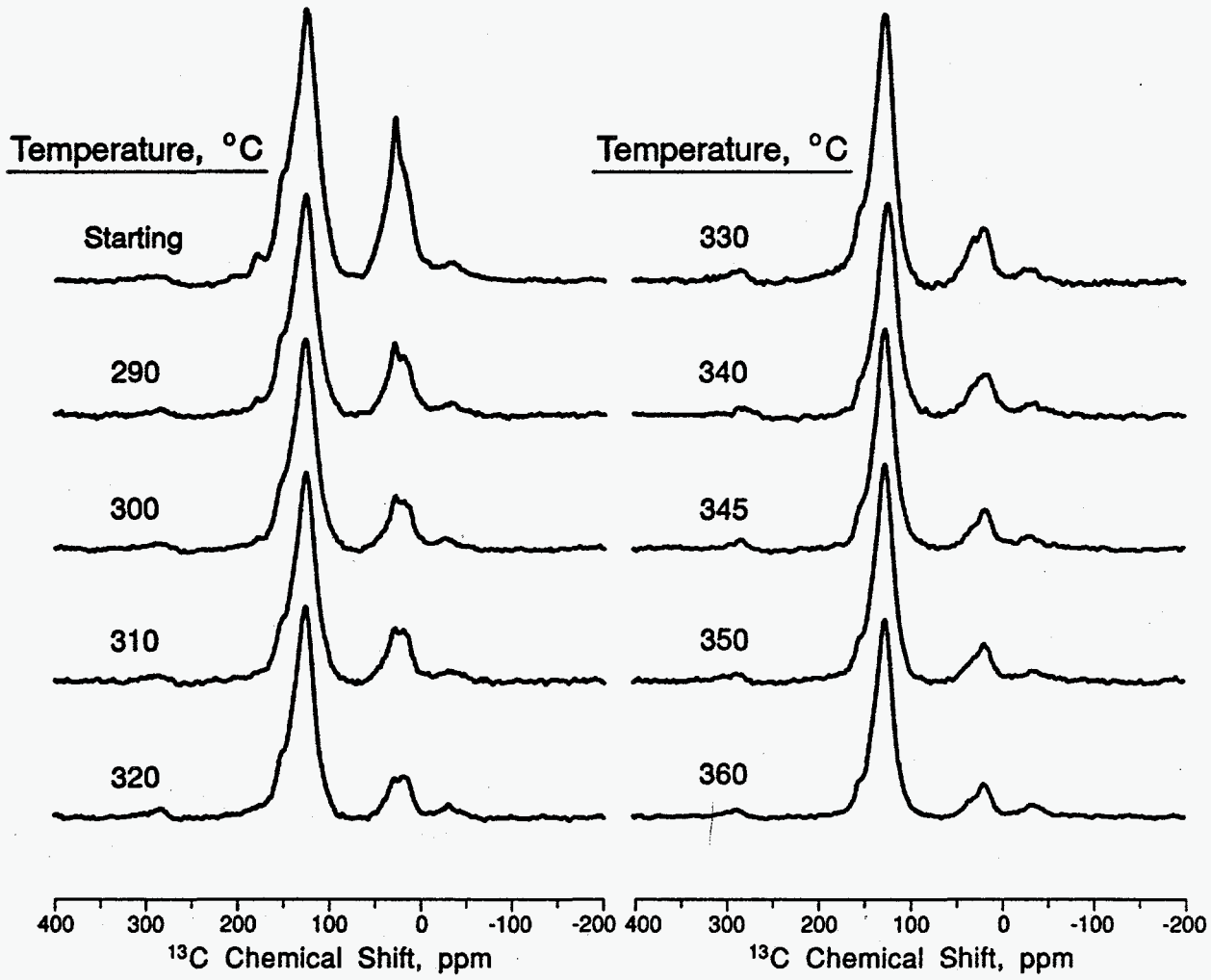

Figure 28. CP/MAS ^{13}C NMR spectra of Lance coal hydrous pyrolysis residues

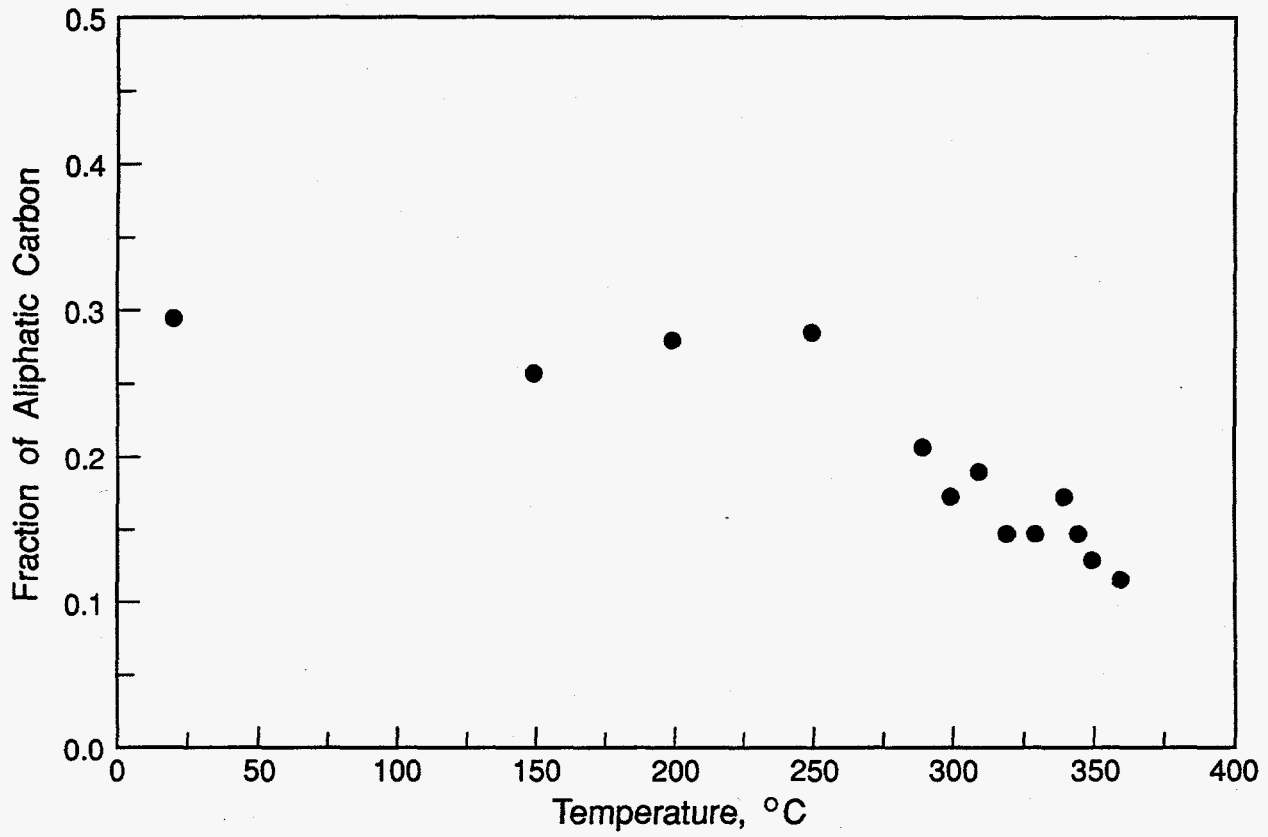

Figure 29. Plot of aliphatic carbon fraction versus hydrous pyrolysis temperature for Lance coal

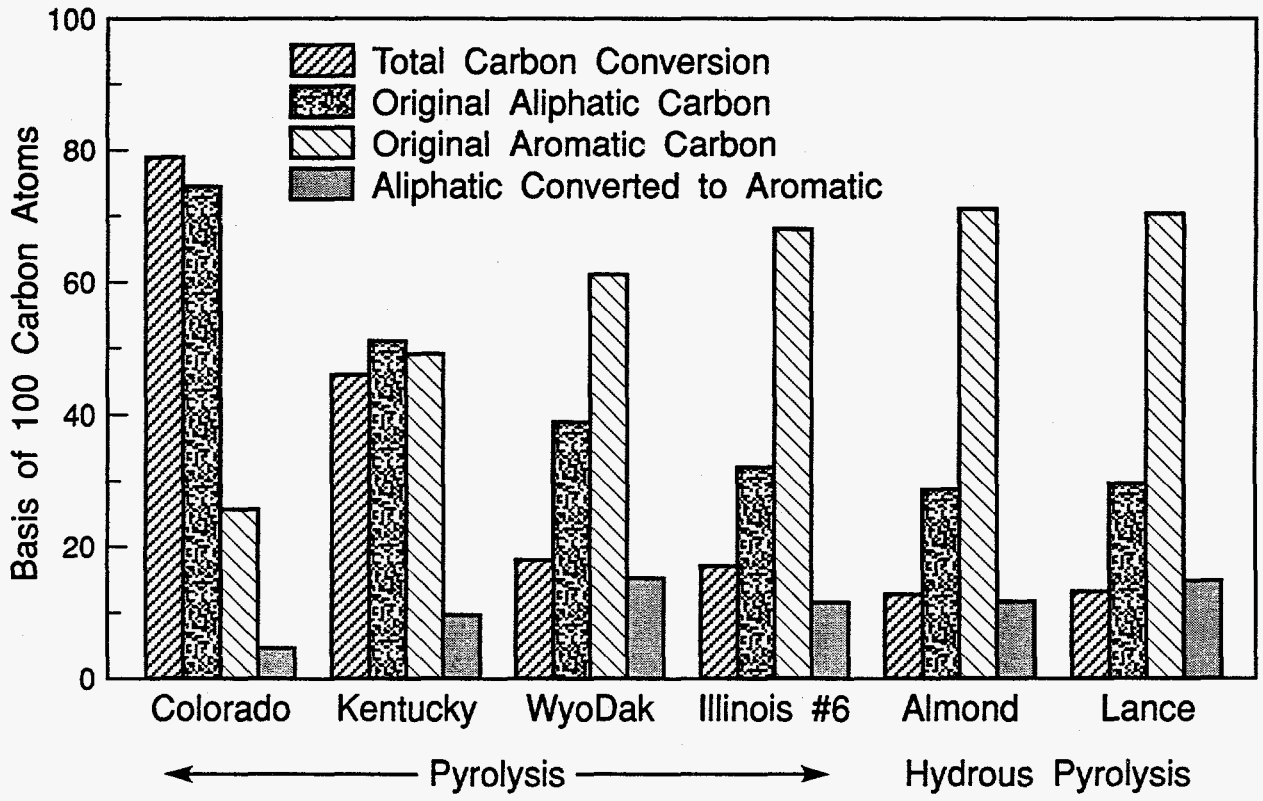

Figure 30. Carbon conversion and aromatization during pyrolysis and hydrous pyrolysis of coals and oil shales

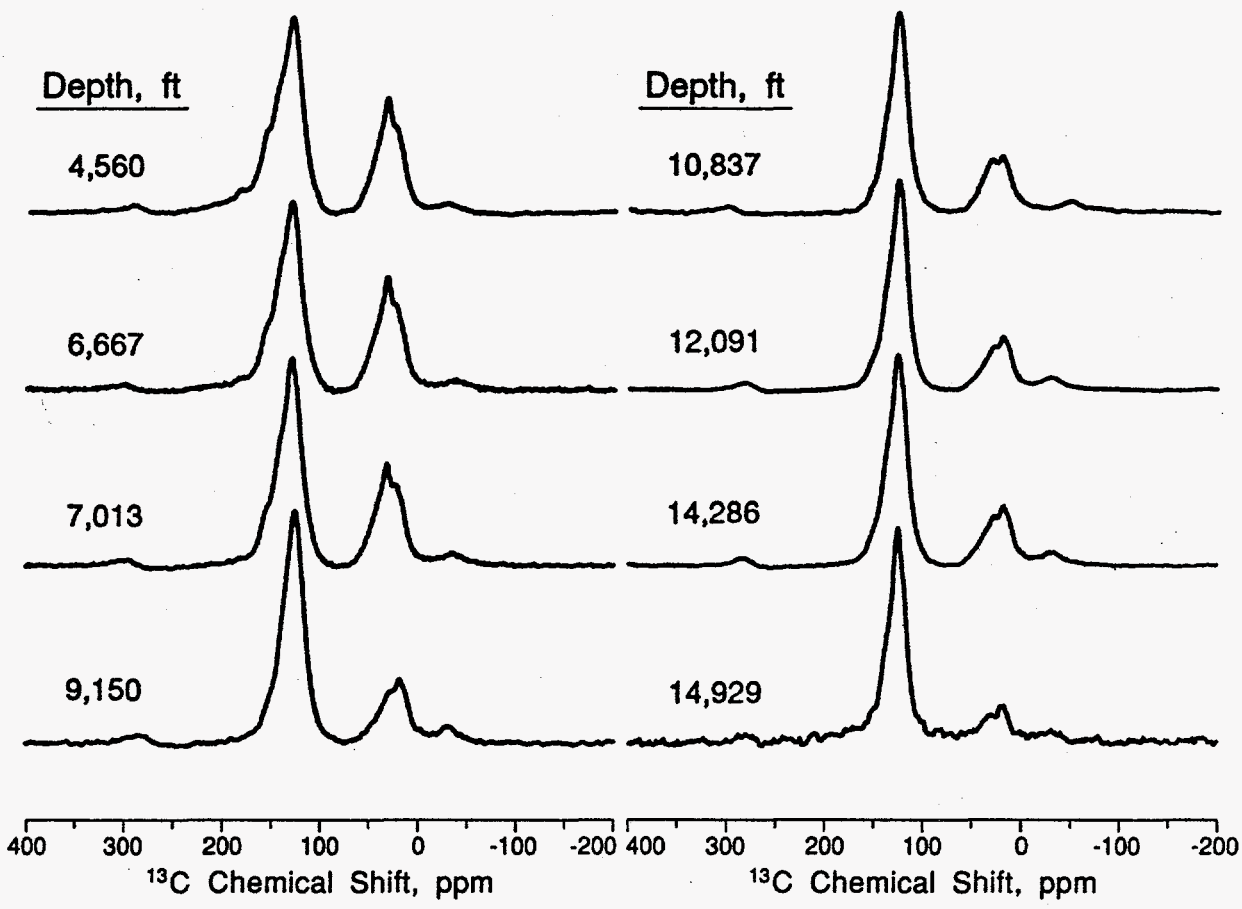

Figure 31. CP/MAS ^{13}C NMR spectra of Almond coals from different depths of burial

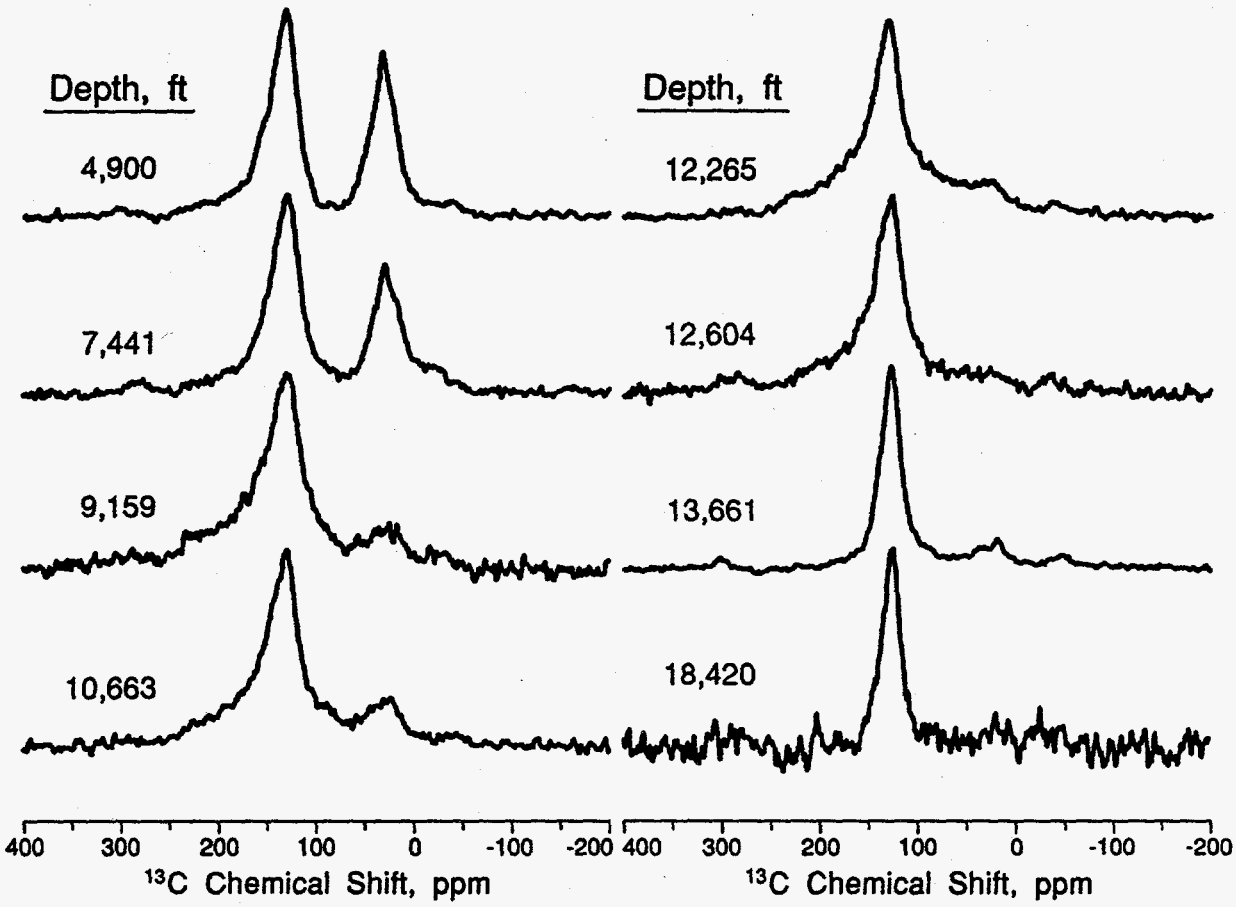

Figure 32. CP/MAS ^{13}C NMR spectra of Almond shales from different depths of burial